Journal of Great Lakes Research 42 (2016) 1212–1227

Contents lists available at ScienceDirect

Journal of Great Lakes Research

journal homepage: www.elsevier.com/locate/jglr

Spatial distributions of external and internal phosphorus loads in Lake Erie and their impacts on phytoplankton and water quality

Hongyan Zhang [a,*], Leon Boegman [b], Donald Scavia [c], David A. Culver [d]

[a] Cooperative Institute of Limnology and Ecosystems Research (CILER), School of Natural Resources and Environments, University of Michigan, Ann Arbor, Michigan 48108, USA
[b] Department of Civil Engineering, Queen's University, Kingston, Ontario K7L 3N6, Canada
[c] Water Center, Graham Sustainability Institute, University of Michigan, 625 East Liberty Road, Ann Arbor, MI 48193, USA
[d] Department of Evolution, Ecology, and Organismal Biology, The Ohio State University, Columbus, OH 43210, USA

ARTICLE INFO

Article history:
Received 8 January 2016
Accepted 3 September 2016
Available online 22 September 2016

Communicated by Joseph DePinto

Index words:
Sediment release
Excretion
Eutrophication
Harmful algal bloom
Hypoxia

ABSTRACT

Re-eutrophication in Lake Erie has led to new programs to reduce external phosphorus loads, and it is important to understand the interrelated dynamics of external and internal phosphorus loads. In addition to developing phosphorus load response curves for algal biomass in the western basin and hypoxia in the central basin, we used a two-dimensional (vertical-longitudinal) hydrodynamic and ecological model to show that both external and internal phosphorus loads were distributed homogeneously in the water column in Lake Erie's western basin. In the stratified central and eastern basins phosphorus released by organic matter decay and crustacean zooplankton excretion was concentrated in the upper water column, contributing 100–119% of the phytoplankton phosphorus demand, while phosphorus released by dreissenids and from anoxic sediments was distributed primarily in the hypolimnion during the growing season. Simulated reductions in external phosphorus loads decreased individual phytoplankton groups most at times when they were normally most abundant, e.g., *Microcystis* decreased the most during September. Phosphorus was limiting over the simulation periods, but water temperature and light conditions also played critical roles in phytoplankton succession. While water column phosphorus responded quickly to external phosphorus reduction, pulses of phosphorus (riverine input or sediment resuspension) occurring immediately before the *Microcystis* bloom period could allow it to bloom despite long-term external phosphorus load reduction. Studies are warranted to assess the contribution of seasonal dynamics in phosphorus loading (including sediment resuspension) to *Microcystis* bloom development.

Introduction

A strong correlation between the concentration of total phosphorus and phytoplankton (hereafter simplified to algae) biomass in freshwater lakes has been well documented (e.g., Lean, 1973; Scavia and Chapra, 1977; Schindler, 1977; Smith, 1982; Knoll et al., 2003), and phosphorus (P) is the most common limiting macronutrient in freshwater lakes (Schindler, 1977; Arnott and Vanni, 1996; Wetzel, 2001; Wilhelm et al., 2003). Excessive P inputs have dramatically increased water productivity and caused the eutrophication of many lakes (Chapra and Robertson, 1977; Beeton, 2002; Jin, 2003; Schindler, 2012).

Lake Erie was severely eutrophic in the 1960s, resulting from excessive external P loading (Burns and Ross, 1972). Water quality management in Lake Erie demonstrated that control of external P loading provides an effective means of decreasing eutrophication. An external P load reduction program for point sources was carried out in the early 1970s, and soon led to encouraging water quality responses. Not only did total phosphorus concentrations decrease in the water column (Rockwell et al., 1989), but total algal biomass decreased 40% in the western basin by the late 1970s, 65% by the mid-1980s, and both Cyanobacteria and filamentous greens decreased by 80% by the mid-1980s (Makarewicz and Bertram, 1991; Gopalan et al., 1998). Oxygen concentrations increased at the bottom of both the western basin (Krieger et al., 1996) and the central basin (Bertram, 1993; Ludsin et al., 2001).

Recent studies show that dissolved reactive phosphorus loads in some tributaries have increased since 1995 (Baker et al., 2014; IJC, 2014; Scavia et al., 2014) and algal biomass has increased as well (Conroy et al., 2005a). In recent years increases in the frequency and magnitude of *Microcystis* blooms (Michalak et al., 2013; Stumpf et al., 2012) suggest that climate may be an additional factor triggering the resurgent blooms, which are correlated with an increased soluble phosphorus fraction from agriculturally dominated tributaries (Kane et al., 2014) and the total phosphorus load from spring freshets (Stumpf et al., 2012). The changes in loads are driven by climate-induced variability in precipitation (Scavia et al., 2014) and are accompanied by trends toward warm, calm meteorology during summer,

* Corresponding author at: 4840 South State Road, Ann Arbor, MI 48108, USA.
E-mail address: zhanghy@umich.edu (H. Zhang).

http://dx.doi.org/10.1016/j.jglr.2016.09.005
0380-1330/

which combine to cause bloom-favorable conditions (Michalak et al., 2013). Consequently, further reduction in the external P load targets has been recommended (Rucinski et al., 2014; Scavia et al., 2014, 2016-in this issue), and the governments of Canada and the United States announced a target of 40% reduction in total phosphorus loads to Lake Erie on February 22, 2016 (USEPA, 2016).

While external loading reduction can reduce symptoms of eutrophication, this result is often delayed by release of internal nutrient loads from years of accumulations and decay of P-rich organic matter in the sediments (Phillips et al., 2005; Turner et al., 2008). Hypoxia in the central basin (and to a lesser extent in the western basin) can cause sediment ferric phosphate deposits to change to the much more soluble ferrous phosphate form, promoting diffusion of soluble reactive phosphate out of the sediments. Another important internal P source to Lake Erie is excretion by zebra mussels (*Dreissena polymorpha* Pallas) and quagga mussels (*Dreissena rostriformis bugensis* Andrusov). These taxa excrete considerable phosphate (Arnott and Vanni, 1996; James et al., 1997) at rates up to 2.8 mg/m^2/d (Conroy et al., 2005b), sufficient to replace the pool of soluble reactive phosphorus (SRP) in the water column in <10 days (Conroy et al., 2005b). However, other studies indicate that dreissenid mussels intercept incoming nutrients in the nearshore area and lead to offshore 'desertification' (e.g., Hecky et al., 2004). The mussel populations retain a large amount of phosphorus in their body tissue (Mellina et al., 1995), which can be released into the water with unclear temporal and spatial patterns. An ecosystem with a high cumulative internal P loading rate from these sources can sustain a eutrophic state well after external P loading has decreased. Thus, the amount and spatial distribution of internal P loading strongly affect the efficiency of any external P reduction program.

In this study, we used Zhang et al.'s (2008) model to simulate the spatial distributions of phosphorus throughout Lake Erie's western, central, and eastern basins during 1997 and 1998. In addition to being the calibration and confirmation years for the model, 1997 and 1998 had higher P loads than the annual target load of 11,000 metric tonnes (mt) and displayed varying *Microcystis* bloom tendencies. Phosphorus loads in 1997 were 16,800 mt with no *Microcystis* bloom, whereas 1998 had lower P loads (12,700 mt) with a moderate *Microcystis* bloom. We evaluated the effects of different reduction levels (20%, 40%, 60%, and 80%) of external total phosphorus loading on algae in the western basin by comparing the biomass of three algal groups with and without reductions in external P inputs to explore years that experience annual external P loads higher than the annual target load of 11,000 mt. We also evaluated the effects of different reduction levels of external total phosphorus loading on hypoxia in the central basin by comparing the hypolimnetic oxygen concentration and hypoxic area with and without reduction in external P inputs, which was similar to the analyses in the multi-model team reports of the Great Lakes Water Quality Agreement Nutrient Annex 4 (Scavia et al., 2016-in this issue; Scavia and DePinto, 2015). Model simulations under different P reduction scenarios provide an overview of the P fluxes and fates in the Lake Erie ecosystem during the summer growing season, and how they respond to external P loads.

Methods

Model description

A two-dimensional (vertical–longitudinal) hydrodynamic and ecological model, EcoLE, was applied to Lake Erie to simulate the effects of external and internal P loading on the Lake Erie ecosystem. The model is an adaptation of the USACE CE-QUAL-W2 version 2 (Cole and Buchak, 1995), with modifications for large lake hydrodynamics (Boegman et al., 2001), multiple algal groups and dreissenid mussels (Zhang et al., 2008). Hydrodynamics and water quality simulations were calibrated and validated in a previous study (Zhang et al., 2008). EcoLE divides Lake Erie into as many as 65 vertical layers at 1-m intervals and 220 longitudinal segments (2-km wide from west to east). The depths of segments were assigned relative to the Great Lakes Datum (GLD) of 1985. State variables in EcoLE include free water surface elevation, horizontal velocity, vertical velocity, water density, water temperature, suspended solids, dissolved organic matter (DOM), particulate organic matter (POM), diatom-derived particulate organic matter (D-POM), soluble reactive phosphorus (SRP), ammonium, nitrate + nitrite, silicon, dissolved oxygen, algal groups (non-diatom edible algae (NDEA), diatoms, and non-diatom inedible algae (NDIA)), cladocerans and four life stages of copepods (eggs, nauplii, copepodites and adults). Data of water temperature and the water quality state variables mentioned above were taken from the Ohio State University's Lake Erie Plankton Abundance Study database to initialize, calibrate and

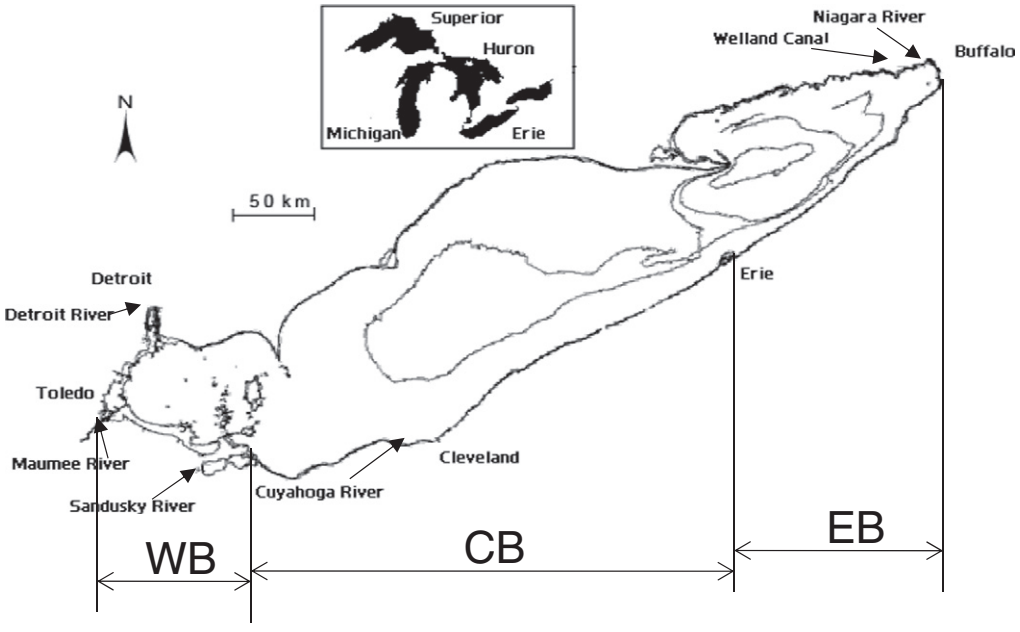

Fig. 1. Locations of tributaries, depth contours of 5, 22, 30 and 50 m, and separations of the Lake Erie western (WB), central (CB) and eastern (EB) basins.

Table 1
TP and SRP loads (metric tons per season) to Lake Erie from tributaries and Waste Water Treatment Plants (WWTP) in 1997 and 1998. Although the seasonal data are listed here, daily/monthly loads were collected and linearly interpolated into every-30- min inputs in the model. Data from D. Dolan, University of Wisconsin-Green Bay, Green Bay, WI, USA, personal communication.

	1997 (May 10–Sep. 30)		1998 (Jun. 10–Oct. 30)	
	TP	SRP	TP	SRP
Maumee River	1221	203	577	143
Toledo WWTP	29	3	26	3
Detroit River	1166	207	891	304
Sandusky River	275	31	168	17
Cleveland westerly WWTP	15	1	13	1
Cuyahoga River	93	12	61	15
Cleveland easterly WWTP	44	4	31	3
Erie WWTP	26	3	21	2
Total	2870	464	1788	487

verify the model. Other data for external driving forces were provided by various sources (Zhang et al., 2008).

Dreissenid mussels were modeled here as external forces, grazing on algae and excreting phosphate and ammonia back into the system. Zhang et al. (2008) used the depth-dependent dreissenid density estimations by Jarvis et al. (2000). However, due to the seasonal hypoxia, low mussel densities were recorded in the deep central basin (Burlakova et al., 2014; Jarvis et al., 2000; Patterson et al., 2005). In this study, we used Jarvis et al.'s density (135 ind/m^2) to populate deep water areas (>22 m) in the central basin. The remaining settings for mussel simulations were kept as in Zhang et al. (2008). We compared the simulation results of before and after the change (see Electronic supplementary materials (ESM) Appendix S1 for details).

The simulation periods were chosen based on availability of field data, and ran from May 10–September 30, 1997 (model calibration) and June 10–October 30, 1998 (model confirmation) (Fig. 1). Using hydrodynamics coefficients based on the Boegman et al. (2001) calibration, our previous modeling efforts with EcoLE focused on the simulation of water temperature, phosphorus and nitrogen, and biomass of algal groups and zooplankton groups over the summer growing season (Zhang et al., 2008). The simulated surface and bottom water temperatures showed good agreement with field observations, and the simulated values of biological and nutrient state variables also matched well with field measurements. Taken together, the simulation results of Boegman et al.'s (2008a) model detailing the interaction between hydrodynamics and dreissenid impacts, and the agreement of state variables (algae, N + N, NH_4 and SRP) between field observations and model predictions (Boegman et al., 2008b), and the simulation results of dissolved oxygen in the western central basin (Conroy et al., 2011) and in the central basin (Scavia and DePinto, 2015), we consider our current model to be a valid analytical tool, which we use herein to study the processes involved in phosphorus recycling in the Lake Erie system under varying external P inputs.

External phosphorus loads

We estimated seasonal external P loads from wastewater treatment plants (WWTP) and non-point sources entering via rivers (Table 1, Fig. 1). Phosphorus load from rivers was measured as soluble reactive phosphorus (SRP) and total phosphorus (TP). SRP was input into EcoLE directly. Although a big fraction of TP from tributaries is inorganic mater, the current model does not simulate the dynamics of inorganic particulate phosphorus. So other phosphorus (TP minus SRP) was converted into phosphorus-containing organic matter assuming organic matter contains 1% phosphorus (Bowie et al., 1985) and was input into EcoLE as organic matter. Because only TP data were available from WWTP, 76.9% of TP was considered as soluble phosphorus and 23.1% was considered as organic matter phosphorus (Young et al., 1982). The external P was assumed to be well mixed in its entrance model cells (i.e., specific segments and layers) and reached other cells by physical or biochemical transport that varied from location to location within the lake. The total external P loads over the simulation periods were calculated as the sum of the products of discharge flow and P concentration in the discharge from each tributary. See ESM Appendix S2 for calculation details. To calculate the external loads' accumulative spatial distributions over the simulation periods, we

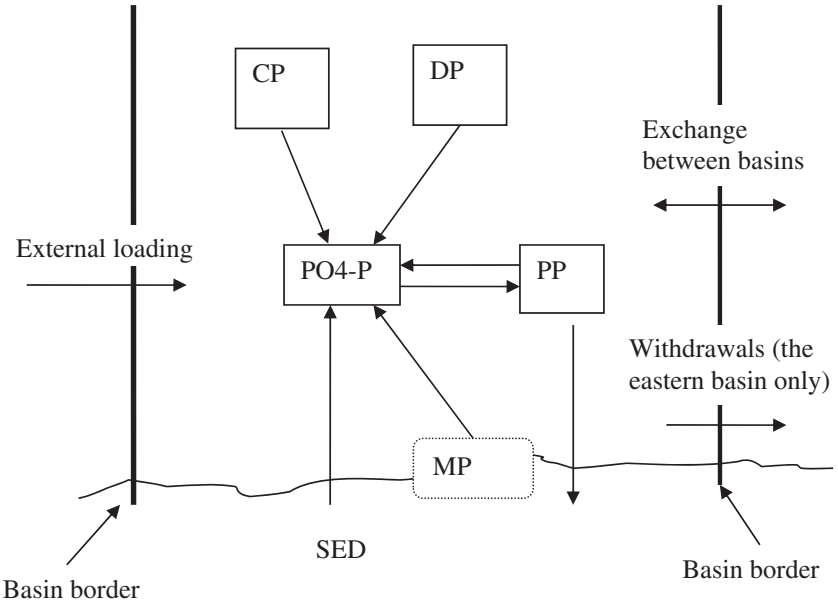

Fig. 2. Basin-wide P pools and cycling pathways incorporated in EcoLE. SRP: soluble reactive phosphorus; DP: P in dissolved organic matter; PP: P in phytoplankton and detritus; CP: crustacean phosphorus content; PP → SRP: phosphorus excretion by phytoplankton and release due to decomposition of detritus; CP → SRP: phosphorus excretion by crustaceans; MP → SRP: phosphorus excretion by dreissenids; SED → SRP: phosphorus release by sediments under anoxic conditions; PP → SED: phosphorus loss to sediment due to sedimentation of PP. Note that these pools and pathways were simulated in each model cell, but are aggregated here to represent basin-wide estimates. External loading: TP loading from tributaries of Lake Erie; Withdrawals: total phosphorus (DP + PP) loss through the Welland Canal and the Niagara River; Exchange between basins: net total phosphorus transported by horizontal currents between basins.

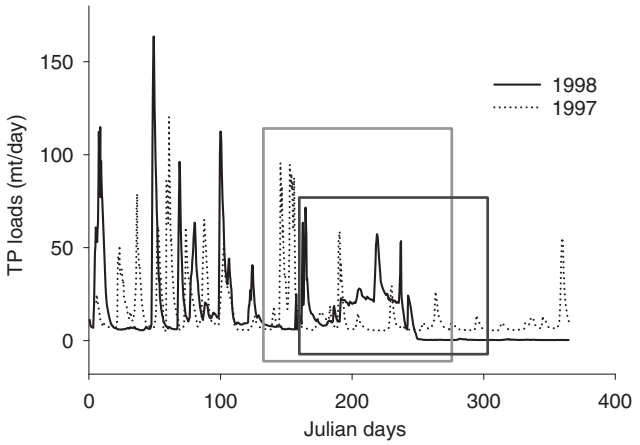

Fig. 3. Total daily phosphorus loads into Lake Erie from the Maumee, Detroit, Sandusky and the Cuyahoga rivers. Data are from the National Center for Water Quality Research, Heidelberg University, Tiffin, Ohio. Note that most of the annual loading occurs by early June in 1997 (outlined by light box), but 1998 had two later high loading events, one in June and the other in July–August (outlined by dark box).

temporarily turned off all the biological and chemical processes in the model, so the resultant spatial distribution results would be exclusively determined by physical transport and mixing processes.

Internal phosphorus loads

Two internal P sources were considered in the model: anoxic sediment release and dreissenid mussel excretion. For comparison, we also considered two phosphorus cycling processes in the water column: crustacean zooplankton excretion (combined excretion from cladocerans and copepods) and organic matter decay. The phosphorus (as SRP) released from these sources was incorporated into the SRP dynamics directly. However, to depict the spatial distribution of phosphorus and track the amount of phosphorus from each source, SRP outputs from the four sources were also recorded as extra state variables. The resultant spatial distributions of SRP from these sources, influenced by physical mixing processes, determined the potential availability from each P source to algal growth.

Anoxic sediment release

Under normoxic conditions, sediments hardly release any phosphorus to the overlying water, whereas they release phosphorus dramatically under anoxic conditions (c.f., Mortimer, 1941, 1971; Burns and Ross, 1972; Di Toro and Connolly, 1980). Lam et al. (1987) assumed that anoxia occurred at 1.5 mg O_2/L (Chapra and Canale, 1991) in the lower layer of their two-layer model, while Burns et al. (2005) considered bottom water anoxic if the epibenthic dissolved oxygen concentration declined to 1.0 mg/L. We adopted Lam et al.'s approach, and assumed that no phosphorus was released when DO concentrations of the bottom water were above 1.0 mg/L, while a constant release rate was used, 0.0044 g P/m^2/d (Lam et al., 1987), when DO concentrations were below 1.0 mg/L. This DO threshold for anoxia was lower than Lam et al.'s (1987), because our deepest water layer was thinner than theirs.

Dreissenid mussel excretion

Zebra mussels first invaded Lake Erie in the late 1980s, but have been more or less replaced by quagga mussels recently (Stoeckmann, 2003, Patterson et al., 2005), such that by 1998, 84.4% of mussels in the eastern basin, 99.7% in the central basin were quagga mussels, but only 36.9% in the western basin (Jarvis et al., 2000). We assume therefore, for simplicity, that during the 1997–1998 periods mussels in the western basin were 100% zebra mussels, whereas those in the central and the eastern basins were 100% quagga mussels. Zebra mussels and quagga mussels have different weight-specific phosphorus excretion rates (Conroy et al., 2005b) and the phosphorus excretion of a mussel population in a model cell over the growing season was calculated as the sum of the products of individual excretion rates and numbers of mussels. See ESM Appendix S2 for the calculation details.

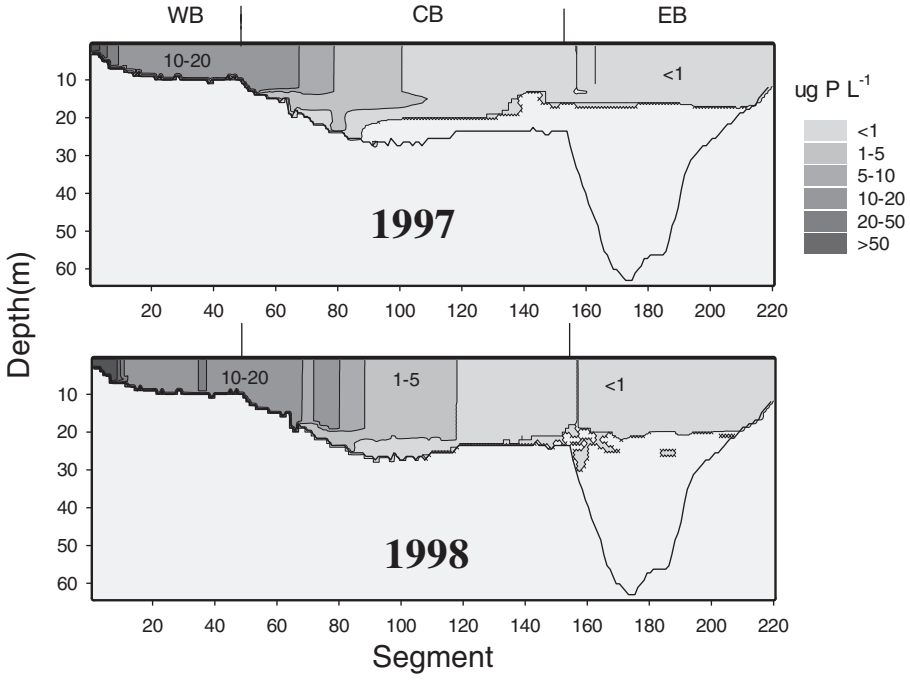

Fig. 4. Comparison of the results of physical transport and mixing processes in the EcoLE model on the spatial distribution of TP entering the lake by external loading during the two years in the study, without involvement of chemical and biological processes. The isopleths show the distribution of TP externally loaded by the end of the two simulation periods (30 September 1997 and 30 October 1998). The x axis represents the 220 2-km spatial segments of the model along the west-to-east axis of the model, whereas the y-axis represents depth in the lake (and the 1-m thick layers of the model). Each segment and layer combination constitutes one cell in this two-dimensional model.

Crustacean zooplankton excretion

We simulated copepods and cladocerans as the two crustacean zooplankters in the lake, using Fennel and Neumann's (2003) stage-structured population model for copepods and a generic bioenergetic model for cladocerans (Zhang et al., 2008). We used a ratio of phosphorus to dry weight ($\delta_{P\text{-}cop}$ for copepods,$\delta_{P\text{-}clad}$ for cladocerans) to convert maintenance cost to phosphorus excretion (Andersen and Hessen, 1991). See ESM Appendix S2 for the calculation details.

Organic matter decay

The organic matter pools (dissolved organic matter (DOM), particulate organic matter (POM) and diatom-derived particulate organic matter (D-POM)) in the water column had temperature-specific decay rates,

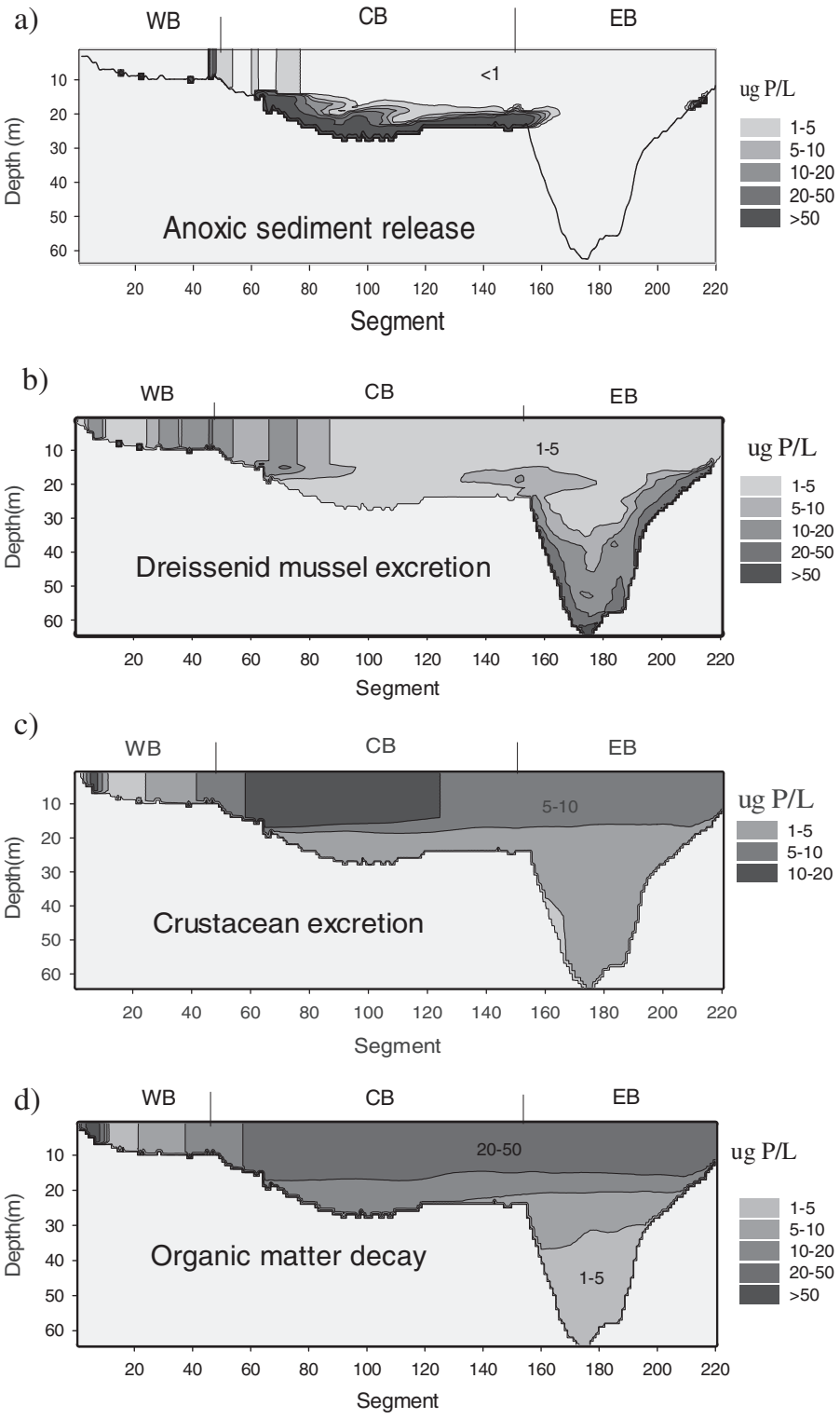

Fig. 5. Comparison of the spatial distribution of SRP from each of the internal sources and the water column cycling processes over the simulation period of 1997, as results of physical transport and mixing processes. The isopleths show the distribution of internally loaded phosphorus on September 30, 1997.

which were converted to phosphorus release rates assuming a ratio of phosphorus to organic matter mass of 0.01 (Bowie et al., 1985). Although phosphorus in DOM is dissolved phosphorus (DP), it is not available directly to algal growth and becomes available through DOM degradation.

Basin-wide phosphorus budget

The phosphorus content of four phosphorus pools: soluble reactive phosphorus (SRP), dissolved phosphorus (DP), particulate phosphorus (PP) and crustacean phosphorus (CP), were estimated basin wide and over the growing season (Fig. 2). DP referred to the phosphorus in dissolved organic matter; PP referred to the phosphorus in particulate organic matter and algae; whereas CP included the phosphorus content of cladocerans and copepods. The pathway from SRP to PP included phosphorus uptake by algae, while PP to SRP included phosphorus excreted by algae and released by POM decay. Our model had a traditional crustacean grazing food web. However, by including organic matter, the model implicitly also includes the microbial food web (Debruyn et al., 2004).

The average mass of each phosphorus pool during the simulation period was calculated as the average sum of the products of the model cell volume and the concentration of phosphorus content of each P constituent in the cell for all model cells across the whole basin. Daily basin-wide phosphorus fluxes between state variables, mussels and sediment were calculated as the daily average of a sum of products of the phosphorus transfer rate from one constituent to another within a model cell and the cell volume for all model cells across the whole basin. See ESM Appendix S2 for the calculation details. To evaluate the effects of reduction in external P loads on the in-lake P dynamics, we calculated the percent changes in the basin-wide P budget for different P reduction scenarios from the no-reduction scenario.

External P loaded to each of the three Lake Erie basins and the exchanges between basins were calculated to complete the P budget. The net P exchanges between connected basins were the sum of the net P fluxes of NDEA-P, NDIA-P, diatom-P, SRP, DOM-P and POM-P. The P exchanges at the intersection between basin separation lines (Fig. 1) were considered as exchanges between basins. Both horizontal advection and diffusion were included.

Table 2
Basin-wide P cycling in 1997, shown as concentrations in major pools and rates of transfer between pools. DP: P in dissolved organic matter; PP: P in phytoplankton and detritus; CP: P in crustaceans; DP → SRP: phosphorus release due to decomposition of dissolved organic matter; PP → SRP: phosphorus excretion by phytoplankton and release due to decomposition of detritus; CP → SRP: phosphorus excretion by crustaceans; MP → SRP: phosphorus excretion by dreissenids; SED → SRP: phosphorus release by sediments under anoxic conditions; PP → SED: phosphorus loss to sediment due to sedimentation of PP. External loading: P loading from tributaries of Lake Erie; withdrawals: total phosphorus (SRP + DP + PP) loss through the Welland Canal and the Niagara River; exchange between basins: net total phosphorus transported by horizontal currents between basins. All values are an average over the simulation period from May 10 to September 30, 1997.

1997		WB	CB	EB	Total
P pools	mt P				
SRP		29.3	710.6	511.0	1250.9
DP		170.3	841.2	434.9	1446.4
PP		176.1	1533.5	433.3	2142.9
CP		14.6	143.8	38.7	197.1
P pathways	mt P/d				
DP → SRP		9.0	33.3	10.2	52.5
PP → SRP		7.4	52.1	12.4	71.9
CP → SRP		3.8	22.3	5.0	31.1
MP → SRP		6.6	6.6	6.3	19.5
SED → SRP		1.2	9.0	0.0	10.2
SRP → PP		24.6	100.0	23.2	147.8
PP → SED		5.2	13.8	3.7	22.7
External loading	mt P/d	15.6	3.1	0.2	18.9
Exchange between basins	mt P/d	−5.9	2.2	3.7	0
Withdrawals	mt P/d			−3.4	−3.4

Effects of phosphorus reduction on algal community in the western basin

To test the effects of a decrease in external P loads on different algal groups for years 1997 and 1998, we reduced the concentrations of SRP, DOM and POM (constituents in tributary loads that contain phosphorus, no algal data were available for the tributaries) by 20%, 40%, 60% and 80% in tributaries without altering flows over the simulation period, which resulted in 20%, 40%, 60% and 80% reductions in external P loads while preserving the seasonal dynamics of the P inputs.

The three modeled categories of algae in Lake Erie were non-diatom edible algae (NDEA), non-diatom inedible algae (NDIA), and diatoms. NDEA included algae of Chlorophyta, Cryptophyta and Pyrrophyta, and were dominated by the genera *Chlamydomonas*, *Oocystis*, *Chroomonas*, *Cryptomonas*, *Rhodomonas*, and *Gymnodinium*. NDIA included algae of Cyanophyta, Pyrrophyta, filamentous Chlorophyta, and were dominated by *Microcystis*. Diatoms were dominated by *Melosira*, *Fragilaria*, and *Cyclotella*. The basin-wide percent differences in the total algal biomass under different levels of external P reduction were calculated as:

$$\frac{B_{lowExtP,t} - B_{ExtP,t}}{B_{ExtP,t}} \times 100$$

where $B_{lowExtP,t}$ was basin-wide total algal biomass at time step t under different reduced levels of external P conditions, while $B_{ExtP,t}$ was under no reduction in the external P loads. We did not provide the percent change in each algal group because when the biomass was low the percent change could overemphasize the effects. Instead, we provided the time series of daily basin-wide algal biomass over the simulation periods for each algal group. We calculated the changes in the monthly-averaged algal biomass for each algal group and the total algal biomass for September, when the peak of *Microcystis* blooms occurred (Bridgeman et al., 2012; Wynne et al., 2010).

Factors influencing the dynamics of algal biomass

In order to analyze in detail the processes that could affect the dynamics of different algal groups, we picked a representative model cell that was located in the western basin close to the Maumee River (segment 5 at 1 m depth), which should show strong effects from changes in the external P loads. We output daily-averaged limiting factors, net growth rates (d^{-1}) (gross growth rate minus excretion rate, mortality rate and settling rate), daily net growth (g DW/m^3/d) (the product of net growth rates and algal biomass), and crustacean zooplankton consumptions (g DW/m^3/d) of different algal groups for this model cell under different levels of external P reductions. In the western basin, all mussels were located on the bottom layer (Zhang et al., 2008), so no mussel grazing occurred in this cell.

Effects of phosphorus reduction on hypoxia in the central basin

Sediment oxygen demand (SOD) is expressed as a function of oxygen concentration and temperature (Lucas and Thomas 1972; Lam et al., 1987).

$$SOD = SOD_{\max} \frac{\Phi_{DO}}{\Phi_{DO} + O_h} \theta^{(T-20)}$$

where $SOD_{\max}$ is maximum sediment oxygen demand at 20 °C, g O_2 m^{-2} d^{-1}, O_h is oxygen concentration half-saturation constant, and Φ_{DO} is the DO concentration in the bottom layer right above sediment. In addition to changes in external P loads, we adjusted the maximum SOD ($SOD_{\max}$) for different TP load scenarios according to the empirical relationship between TP loads and SOD developed by Rucinski et al. (2014, Scavia and DePinto, 2015). To calculated hypoxic area (area with DO <2 mg/L), we used Zhou et al.'s method (Zhou et al., 2013), which

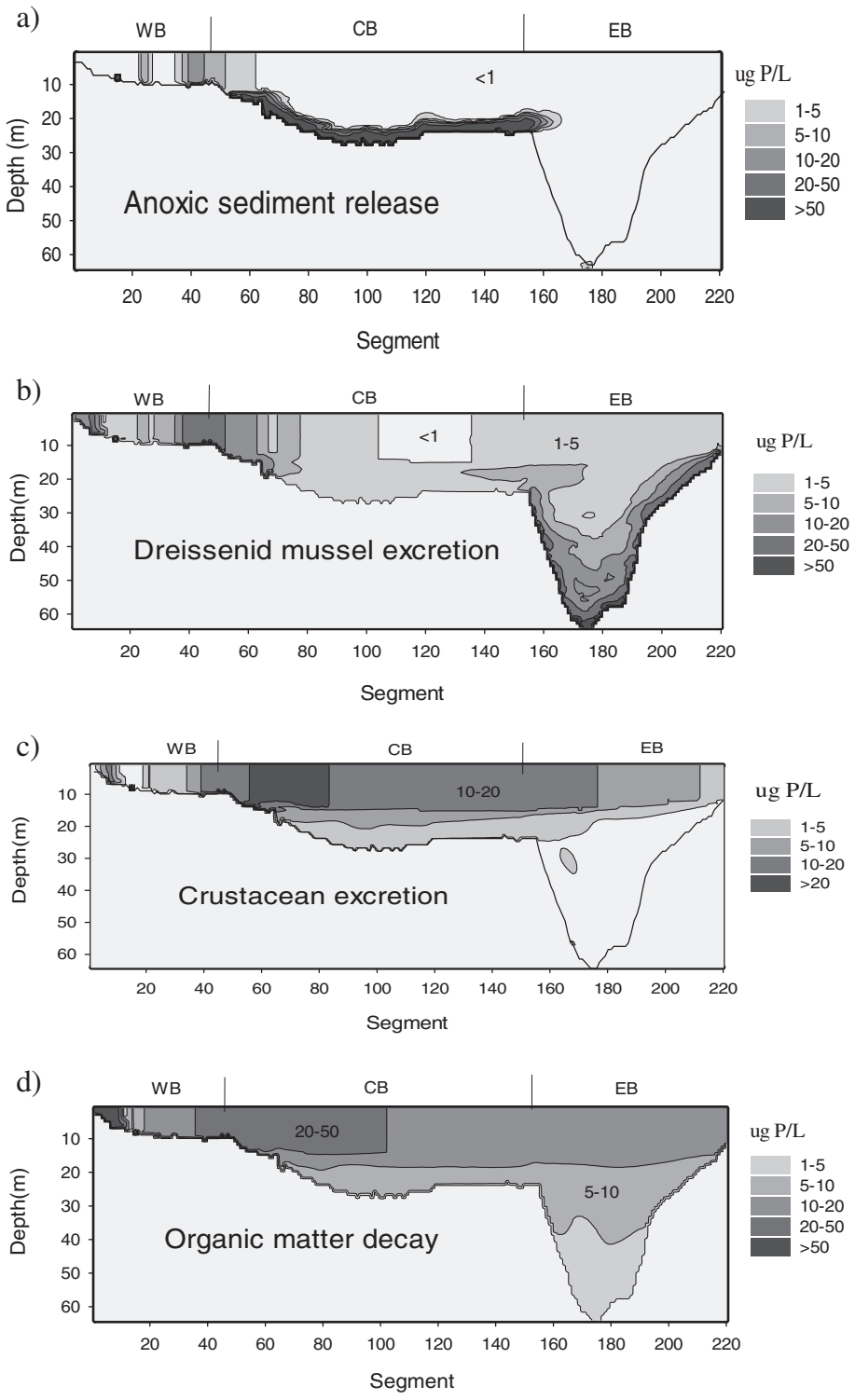

Fig. 6. Comparison of the spatial distribution of SRP from each of the internal sources and the water column cycling processes over the simulation period of 1998, as results of physical transport and mixing processes. The isopleths show the distribution of internally loaded phosphorus on October 30, 1998.

was based on the average of bottom dissolved oxygen concentration (DO) measured from 10 monitoring stations by U.S. Environmental Protect Agency every fall. Our bottom DO (1–3 m above the sediment) was averaged among model segments that corresponding to the 10 monitoring stations from August 1 to September 30, 1998, a year that had an annual TP phosphorus load close to that of 2008. We then converted these DO concentrations to hypoxic area using Zhou et al.'s empirical relationship for each TP reduction scenario.

Results

External phosphorus loads

The total phosphorus loaded into Lake Erie from tributaries during the simulation periods was primarily from the Maumee and the Detroit Rivers, whereas loads from waste water treatment plants were relatively small (Table 1). Temporally, most of the external P loads occurred

Table 3
As Table 2, but for June 10 through October 30, 1998.

1998		WB	CB	EB	Total
P pools	mt P				
SRP		42.3	1061.5	826.1	1929.9
DP		158.0	621.9	259.8	1039.7
PP		392.0	1492.5	481.4	2365.9
CP		21.0	134.8	19.6	175.4
P pathways	mt P/d				
DP → SRP		8.8	29.5	9.8	48.1
PP → SRP		14.4	51.2	15.4	81.0
CP → SRP		5.4	21.2	2.0	28.6
MP → SRP		6.3	6.8	6.3	19.4
SED → SRP		2.3	11.8	0.0	14.1
SRP → PP		33.7	102.3	25.9	161.9
PP → SED		11.7	10.9	3.3	25.9
External loading	mt P/d	10.2	2.1	0.1	12.4
Exchange between basins	mt P/d	−7.4	2.8	4.6	0
Withdrawals	mt P/d			−2.8	−2.8

during early summer (Julian days 131–160) in 1997, while a big fraction of external P load occurred during summer 1998 (Julian days 190–240) (Fig. 3). Spatially, the model depicts that most of the external P loads, under pure advection and physical mixing processes, were concentrated in the western and west-central basins (Fig. 4), and contributed little to the phosphorus concentrations in the east-central and eastern basins.

Spatial distribution of internal phosphorus loads

We used specific state variables to track the phosphorus from each of the two internal P sources and the two water column cycling processes. The tracked phosphorus was accumulated in the water column and distributed fully by the physical mixing process. Here, we report the resultant phosphorus concentration distributions from different P sources at the end of September.

Anoxic sediment released phosphorus primarily at the bottom of the central basin over the simulation period (Fig. 5a). Sediment phosphorus was trapped in the hypolimnion by thermal stratification and showed little influence on the epilimnion phosphorus concentration during the growing season. Because sediment only releases phosphorus when it is under anoxic conditions, the sediment phosphorus release profiles also reflect the simulated oxygen conditions on the lake bottom.

Dreissenid mussels excreted a total amount of phosphorus higher than that of zooplankton in the western basin (Table 2). Dreissenid excretion resulted in 5–20 μg P/L in the upper water in the western and the west-central basins, while it resulted in <5 μg P/L in the upper water in the rest of the lake (Fig. 5b). Very low dreissenid excretion occurred in the central basin, which experiences seasonal hypoxia. In the stratified eastern basin, most of the phosphorus was concentrated in the lower water column.

Vertically, crustacean excretion was concentrated in the water column with depths of 20 m and shallower in 1997 (Fig. 5c). Horizontally, crustacean excretion contributed the highest fluxes in the segments

Table 4
Percent changes in the phosphorus pools and pathways under different reduction levels in the external phosphorus loads at the end of September of 1997.

1997	WB				CB				EB			
	20%	40%	60%	80%	20%	40%	60%	80%	20%	40%	60%	80%
P pools												
SRP	−7	−12.1	−18	−29	0	−0.6	−1.5	−2.7	0	−0.1	−0.1	−0.2
DP	−19.8	−39.2	−58.7	−78.4	−1.8	−3.6	−6.3	−11.2	−0.3	−0.5	−0.9	−1.3
PP	−18.9	−33.1	−46.9	−61.5	−1.2	−2.6	−4.3	−8.8	−0.1	−0.3	−0.6	−0.9
CP	−26.9	−50.5	−73.7	−93.6	−2.5	−5.6	−11	−16.5	−0.2	−0.4	−0.9	−1.2
P pathways												
DP → SRP	−19.8	−39.1	−58.6	−78.4	−1.8	−3.7	−6.5	−11.7	−0.4	−0.8	−1.4	−2
PP → SRP	−18.7	−32.6	−46.1	−60.3	−1.3	−2.9	−5	−9.9	−0.1	−0.4	−0.7	−1.1
CP → SRP	−21.8	−46.1	−73.2	−94.4	−2.2	−5	−12.7	−22.7	−0.3	−0.6	−1.2	−1.7
MP → SRP	0.2	0.8	2	3.2	0.3	0.7	1.6	3	0	0	0	0
SED → SRP	−6.3	−14.6	−20	−27.9	0	−0.4	−0.6	−1.4	1.6	−2.9	−0.6	0.4
SRP → PP	−16.3	−31.1	−46.7	−61.7	−1.3	−2.9	−5.6	−10.9	−0.2	−0.5	−0.9	−1.4
PP → SED	−17	−29.5	−40.3	−51.1	−1.5	−2.9	−5	−10.3	0	−0.1	−0.5	−0.7

Table 5
Percent changes in the phosphorus pools and pathways under different reduction levels in the external phosphorus loads at the end of September of 1998.

1998	WB				CB				EB			
	20%	40%	60%	80%	20%	40%	60%	80%	20%	40%	60%	80%
P pools												
SRP	−28.7	−46.4	−56.2	−64.1	−0.9	−1.4	−1.8	−2.4	−0.1	−0.1	−0.1	−0.1
DP	−22.1	−43.4	−62.2	−79.6	−5.6	−10.1	−14	−18.2	−0.4	−0.5	−0.9	−1.2
PP	−22.7	−41.1	−52.4	−65.6	−2.5	−4.3	−5.4	−6.6	−0.2	−0.1	−0.4	−0.5
CP	−14.8	−38.7	−66.7	−88.3	−3	−5.4	−8.2	−12.3	−0.1	−0.2	−0.6	−0.6
P pathways												
DP → SRP	-21.8	−43.2	−62	−79.5	−6.1	−10.9	−15.1	−19.6	−0.5	−0.7	−1.3	−1.7
PP → SRP	-22.5	−40.8	−51.5	−64.5	−2.9	−4.8	−6	−7.4	−0.2	−0.2	−0.4	−0.5
CP → SRP	-17.5	−39.4	−62.9	−86	−4.9	−8.3	−11.1	−15.8	−0.4	−0.5	−1.1	−1.1
MP → SRP	6.3	10.2	11.9	12.3	0.8	1	1.2	1.4	0	0	0	0
SED → SRP	-41.4	−73.1	−80.8	−86.1	−0.1	−0.3	−0.7	−1.7	−0.2	−2.4	0.9	−0.8
SRP → PP	-16.3	−31.1	−46.7	−61.7	−1.3	−2.9	−5.6	−10.9	−0.2	−0.5	−0.9	−1.4
PP → SED	-17	−29.5	−40.3	−51.1	−1.5	−2.9	−5	−10.3	0	−0.1	−0.5	−0.7

close to the Maumee River mouth (segments 1–11) and in the western central basin. By the end of September, crustacean excretion resulted in a SRP concentration in the water column as high as 20 μg P/L in 1997 (Fig. 5c). The phosphorus excreted by crustaceans in the western basin between segments 12 and 24 (east of the segments influenced by the Maumee River) was extremely low, which illustrates the influence of the Detroit River's high flows and low phosphorus content. The phosphorus released by organic matter in 1997 was also concentrated in segments 1–11 that were close to the Maumee River and in the upper water column of the central and eastern basins, where it resulted in up to 50 μg P/L by the end of September (Fig. 5d).

Spatial distributions of these four P sources in 1998 were similar to those of 1997 (Fig. 6). However, the zooplankton excretion of phosphorus in 1998 contributed little to the deep water phosphorus content in the eastern basin compared to 1997 (Figs. 5c and 6c). Organic matter decay resulted in a lower phosphorus concentration in eastern Lake Erie compared to that in 1997 (Figs. 5d and 6d), consistent with the lower external nutrient loads in 1998 than in 1997.

Basin-wide phosphorus budgets

Particulate phosphorus (PP) was the largest phosphorus pool, with an average of 2143 mt in the lake in 1997 and 2366 mt in 1998 (Tables 2–3). SRP in the central and eastern basins was similar to, or larger than dissolved organic phosphorus (DP), but was much lower than DP in the western basin. The zooplankton phosphorus pool was the smallest phosphorus pool among the four, and was less than one-tenth of the other particulate phosphorus pool.

The model showed that the most active phosphorus pathway was from SRP to PP, due to the active phosphorus uptake by algae in all three basins for both years (Tables 2–3). Algal uptake could deplete the western basin SRP pool within 2 days, while the phosphorus regenerated daily in the water column by organic matter and zooplankton excretion was 82–85% of the western basin algal demand, with 26–36% from DP, 30–43% from PP, and 16% from crustaceans. Dreissenid mussels could provide 19–27% of the algal P demand each day. In the central and eastern basins, the P regenerated daily in the water column by organic matter and zooplankton excretion was 100–119% of the algal demand, with 78–97% from organic matter decay. Dreissenid mussels could provide 7% of algal P demand in the central basin and 24–27% in the eastern basin, but it only becomes available to algae after fall turnover starts. The sums of organic matter decay, zooplankton excretion, mussel excretion and sediment release were similar to the total algal uptake in all three basins, indicating fast recycling of phosphorus in the water column (Tables 2-3).

In the western basin, the daily external P loads were three times higher than P sedimentation in 1997, but slightly smaller than P sedimentation in 1998. Phosphorus pathways within the water column (e.g., SRP → PP and PP → SRP) and P exchange between western basin and central basin were greater in 1998 than those in 1997, which suggested that when nutrient loads were lower, phosphorus recycled faster within the water column. The total P input to the water column (sum of external P, sediment release and mussel excretion) was higher than P loss to the sediment in both years. Western basin sediment release indicated that anoxic conditions occurred during the simulation period (Loewen et al., 2007). External loads to the central and eastern basins were small compared to their internal loads, while sediment release

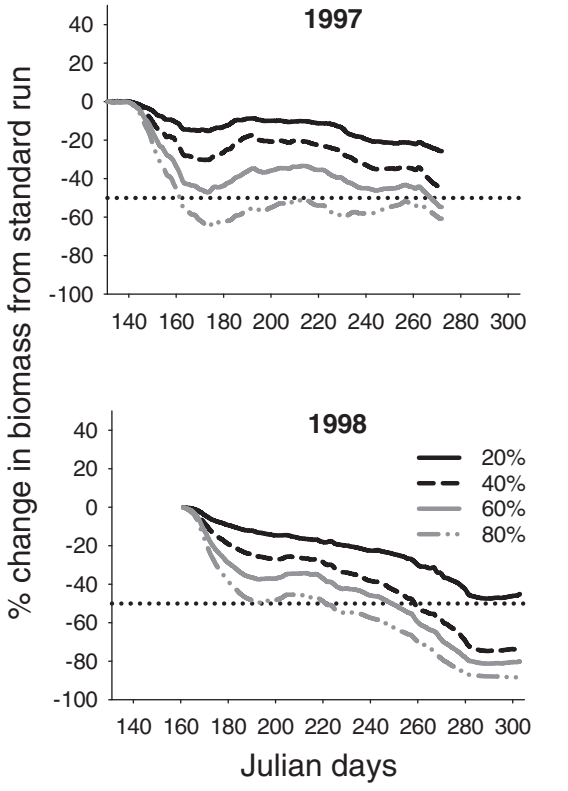

Fig. 7. Percent change of total algal biomass over the simulation periods for 1997 and 1998 under different levels of external phosphorus loading reduction (decrease by 20, 40, 60 and 80%) from model runs with no reduction (standard run). The dotted lines indicate a 50% decrease in algal biomass.

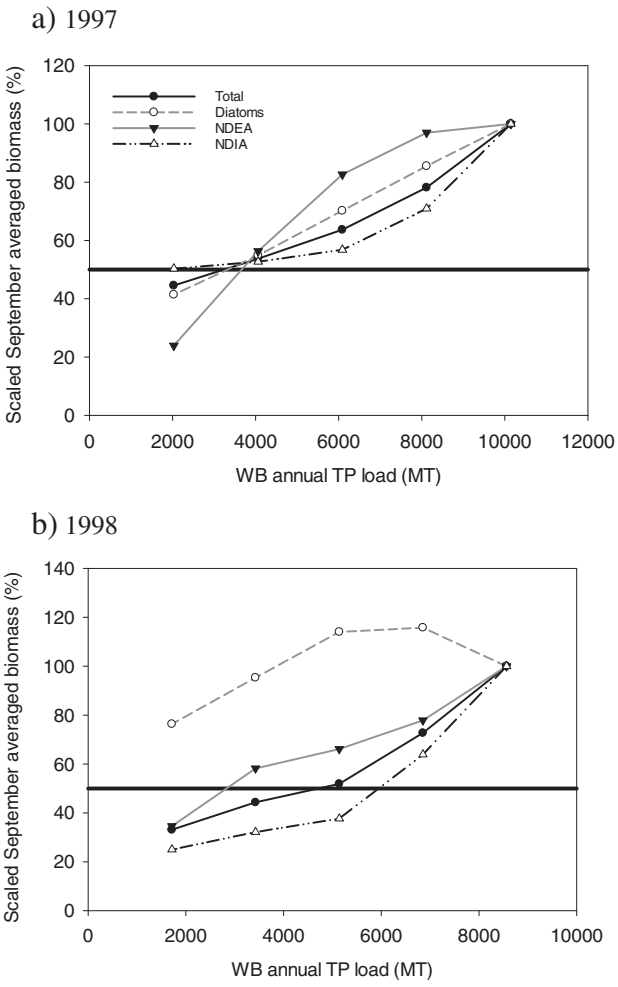

Fig. 8. September-averaged biomass for total algae, and three algal groups for 1997 and 1998 under different levels of external phosphorus loads to the western basin. Biomass was scaled to the biomass with no phosphorus reduction. The horizontal line represents a 50% reduction relative to model runs with no reduction.

was the largest P input to the water column for the central basin and mussel excretion was the largest P input to the water column for the eastern basin. The difference between external loading and withdrawals from the Niagara River and Welland canal showed that the lake retained 77–82% of the total external P loads; some of which is lost to sedimentation.

Under the four P reduction scenarios, large changes in P pools and fluxes occurred in the western basin, less in the central basin, and essentially no change in the eastern basin for both years (Tables 4-5). The SRP pool in 1997 was reduced by less than the percent reduction in external P loads (Table 4), but decreased more in line with the reduction of the external loads in 1998 (Table 5). In the western basin, decreases in the water column fluxes were much larger than those on the bottom, while mussel excretion increased due to improved oxygen conditions (Tables 4–5). However, our simulations were limited by fixed mussel excretion rates, while in reality mussel P excretion should be a function of phosphorus ingested from grazed algae (Vanderploeg et al., in review), which, in turn, should be a function of the external loads. Consistent between the two years, most phosphorus pools and fluxes decreased in proportion to the reduction of the external P loads,

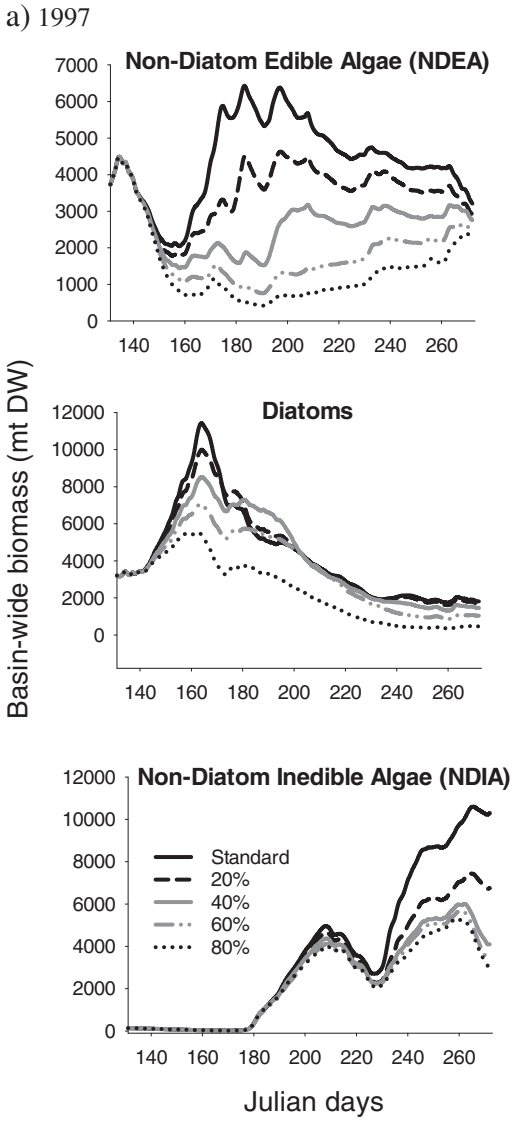

Fig. 9. Time series of biomass (mt DW) for three algal groups over the simulation periods of a) 1997 and b) 1998 under different levels of reduction in external phosphorus loading (decreased by none, 20, 40, 60 and 80%). Note the different scales on the y-axes.

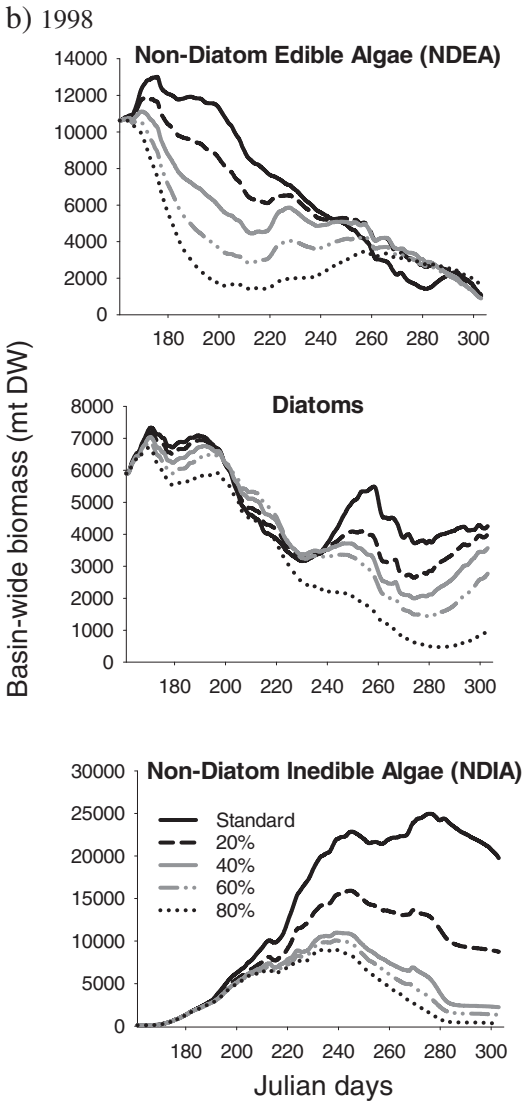

Fig. 9 (*continued*).

except zooplankton biomass decreased by percentages higher than the reductions in the external P loads.

Effects of phosphorus reduction on the algal community in the western basin

Upon simulation of reductions of 20%, 40%, 60%, and 80% of external P loading in the western basin, the total algal biomass decreased more under the higher reduction scenarios. In the 80% P reduction scenario, the total algal biomass decreased by up to 65% during late June of 1997 and leveled off thereafter, while it decreased gradually by 88% from June to October in 1998 (Fig. 7). NDIA decreased more than other algal groups during September under most TP reduction scenarios, except when the TP reduction amount was large (>60%) in 1997 and NDIA biomass was already low (Fig. 8).

A clear algal succession pattern occurred in 1997, where diatoms peaked in early June when temperature was still cool and optimal for diatom growth, then NDEA became dominant with favorable high water temperatures, followed by an increase in NDIA in August (Figs. 9a, 10). In 1998, nutrient loads during summer boosted the growth of NDIA (Figs. 3, 9b), while NDEA and diatoms decreased due to competition for light (Fig. 11b).

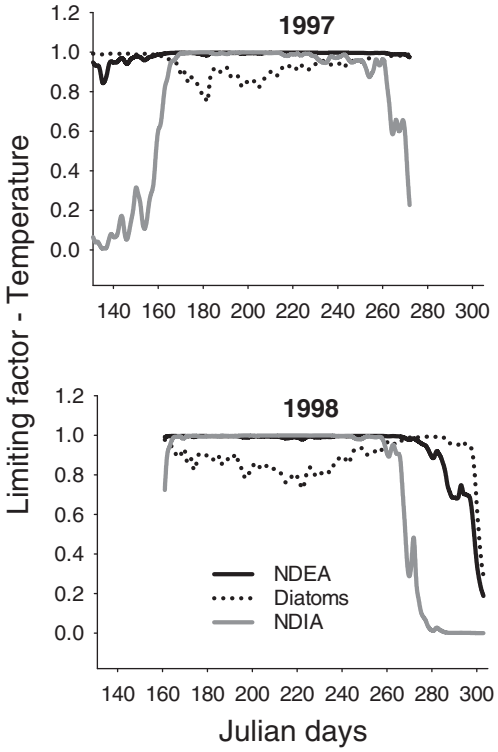

Fig. 10. Limiting factor of water temperature (dimensionless) on the growth of three algal groups in a typical model cell close to the Maumee River in the western basin (segment 5 and 1 m below the water surface) for a) 1997 and b) 1998.

Phosphorus loading reduction simulations predict large decreases in the algal groups with the highest biomass. NDEA decreased during its peak time in late June–July (Julian days 170–220) by as much as 93% in 1997 (in the 80% reduction scenario) and as much as 85% in 1998. Diatoms showed a large decrease during the period when water temperature was optimal for diatom growth and were less affected by the P reduction during hot periods (Figs. 9, 10). NDIA biomass was low in 1997 and decreased by 20% until later in August, when NDIA biomass was high and the decrease in biomass became larger (by up to 69%) with phosphorus loading reductions, while NDIA was abundant in 1998 and decreased by up to 97%.

Factors influencing the dynamics of algal biomass

For the representative model cell close to the Maumee River in the western basin (segment 5 and at 1 m depth), we output detailed calculated results relevant to algal dynamics, including limiting factors of water temperature, light, nitrogen, phosphorus, silicon for diatoms, algal daily respiration, excretion, senescence mortality, sedimentation and gross growth rate (d^{-1}), plus crustacean zooplankton grazing mortality on NDEA and diatoms.

Different algal groups had different water temperature preferences, with diatoms favoring cooler temperatures, NDIA favoring warm temperatures and NDEA in between (Fig. 10). The temperature influence on algal growth was not affected by the reduction of external P loads. Nitrogen was not a limiting factor for any of the three groups, and silicon was not a limiting factor for diatoms over the simulation periods in this model cell. However, the effects of light and phosphorus on algal groups were changed under different levels of P reduction. Phosphorus loads can strongly decrease the light conditions for the growth of NDEA and

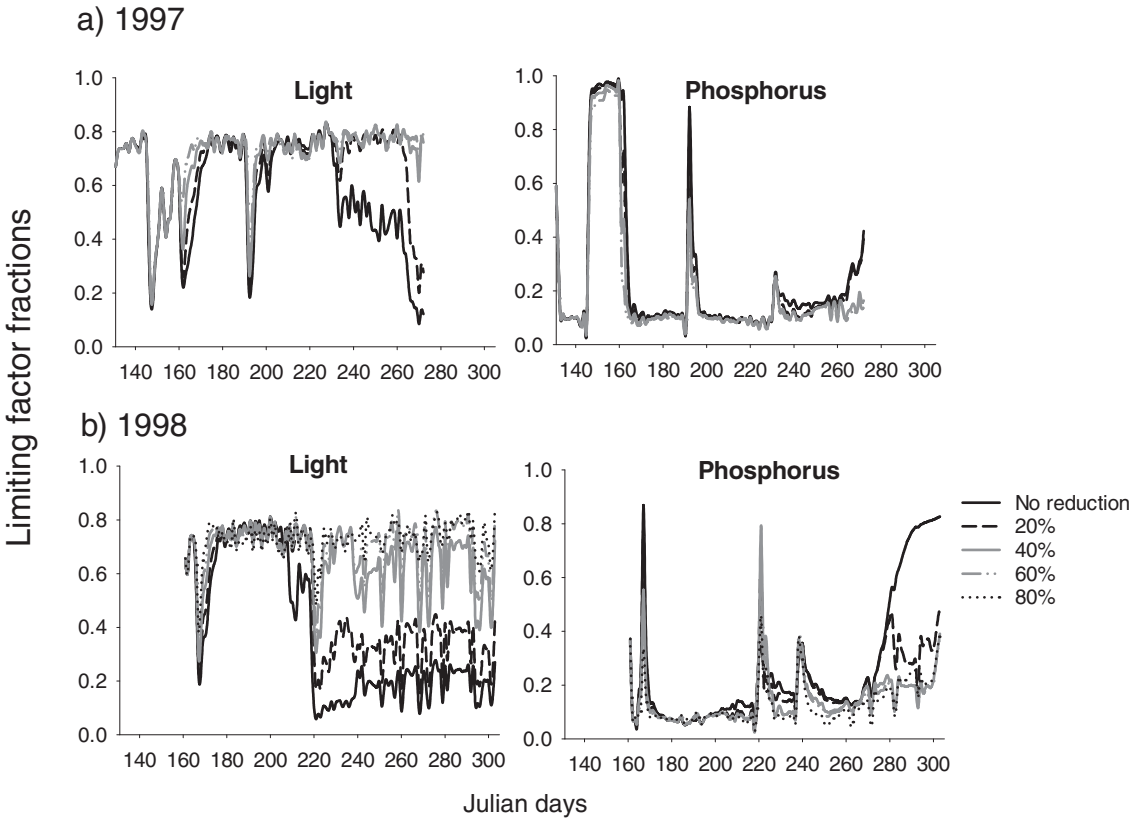

Fig. 11. Limiting factors (dimensionless) calculated based on light and phosphorus for NDEA and diatoms in the typical model cell for a) 1997 and b) 1998 under different phosphorus fractional reduction scenarios (no reduction, reduction of 20%, 40%, 60% and 80%). NDEA and diatoms were affected by light and phosphorus in the same way.

diatoms, especially when the P loading events were followed with fast growth of NDIA (Figs. 11, 12a). In 1998, after an increase of nutrients around Julian day 220, NDIA had a strong growth pulse, and the light conditions for NDEA and diatoms replaced phosphorus to become a limiting factor. Reduction in P loads led to decreases in NDIA and increases in light conditions for NDEA and diatoms. This explains why NDEA biomass was higher under P reductions later during the simulation period of 1998 (Fig. 9b).

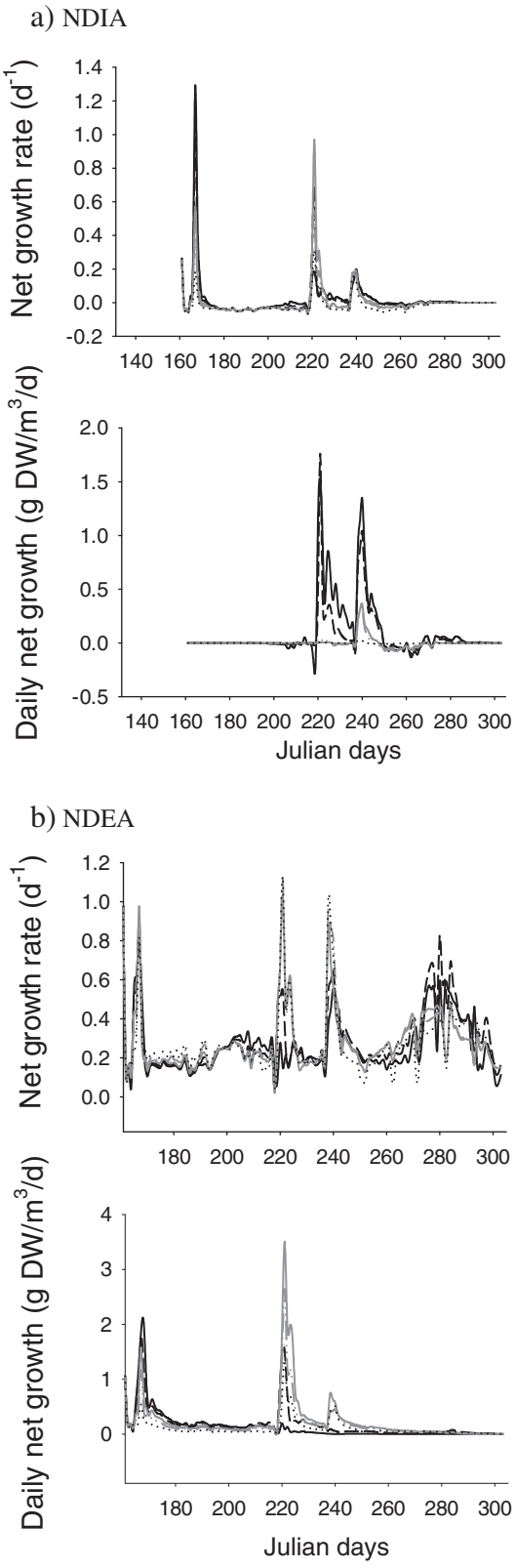

Fig. 12. Daily net growth rate (d^{-1}) and net growth (g $DW/m^3/d$) over the simulation period of 1998 for a) non-diatom inedible algae NDIA, b) non-diatom edible algae NDEA, and c) diatoms under different phosphorus reduction scenarios (no reduction, reduction of 20%, 40%, 60%, and 80%). Note the different scales on the y-axes.

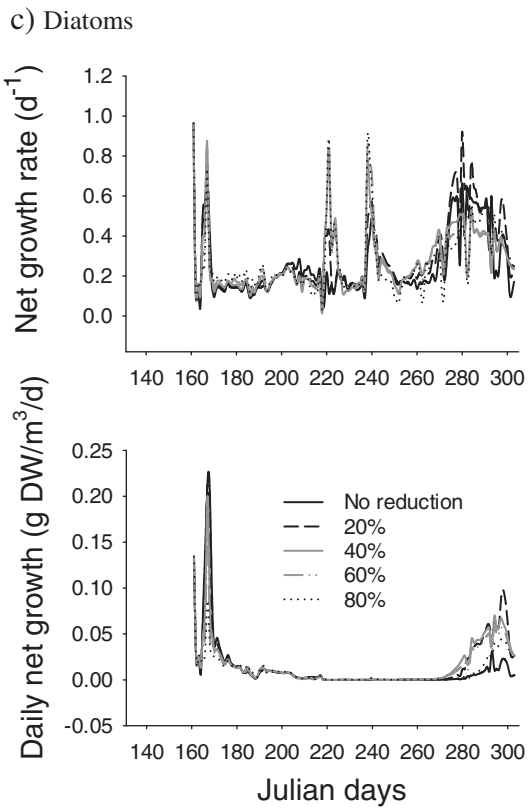

Fig. 12 (*continued*).

Although algal daily respiration, excretion, and senescence mortality rates were much smaller than the gross growth rate, especially when gross growth rates were high, under lower gross growth rates, net growth rates can be negative (Fig. 12a). Although NDEA and diatoms had similar net growth rates (d^{-1}), their individual realized daily growth rates (g $DW/m^3/d$) differed as did the curves of the net growth rates (d^{-1}, Fig. 12b–c). The realized daily growth rates were defined by the current algal biomass. NDIA biomass was very low at the beginning of simulations, and gained little biomass daily before Julian day 200 even with a big growth rate around Julian day 170 (Fig. 12a). However, nutrient loads after Julian day 220 obviously enhanced the growth of NDIA for both 1997 and 1998, especially in 1998 (Fig. 12a). Sedimentation and crustacean grazing mortality on NDEA and diatoms were proportional to the current biomass.

Effects of phosphorus reduction on hypoxia in the central basin

With no TP reduction, the average hypolimnetic DO concentration in the central basin in 1998 was 1.6 mg/L, and the hypoxic area was 6435 km^2 (Fig. 13). Hypoxia in the central basin improved with decreased TP load, until TP load was decreased below 4000 MT with hypoxia declining rapidly with TP reduction.

Discussion

The cause–effect relationship between external P loads and harmful algal blooms (e.g., *Microcystis* blooms) in Lake Erie has been reevaluated

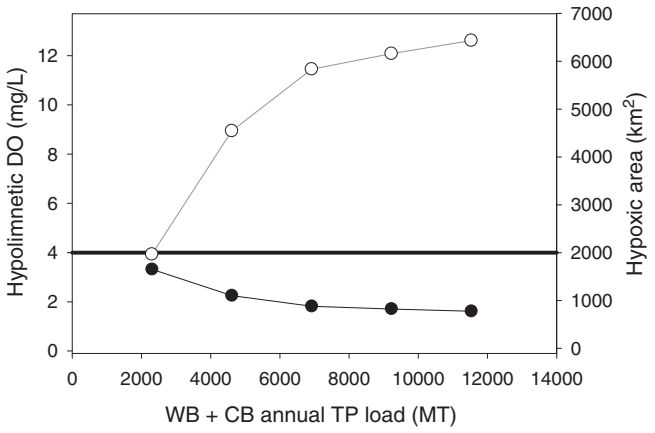

Fig. 13. Relationships between total TP load to the western and central basins and hypolimnetic DO (black line) and hypoxic area (gray line) for model year 1998. The reference line indicates the hypolimnetic DO concentration of 4 mg/L, and a threshold hypoxic area of 2000 km^2.

and confirmed recently (Kane et al., 2014; Obenour et al., 2014; Stumpf et al., 2012; Verhamme et al., 2016-in this issue). In addition to the increasing soluble phosphorus in external P loads, the ongoing changes in land use, agricultural practices and climate change also favor the re-eutrophication of Lake Erie (Michalak et al., 2013; Scavia et al., 2014). The phosphorus loading target that once improved water quality in the 1970–80s will not be good enough to maintain water quality now and in the future (Scavia et al., 2014). A new external P loading target of a 40% decrease from current levels was announced as part of an adaptive management plan (US EPA, 2016). Our study provides some scientific insight and support for this further P reduction. Using a process-oriented mathematical model to depict the spatial distribution of both external and internal loads, we estimated the sizes of basin-wide P pools and pathways to determine the relative importance of different P sources and availability to algal growth. We also simulated responses of three algal groups to different levels of phosphorus reduction, which advances most of the research on eutrophication of Lake Erie that only addressed a single model algal group (IJC, 2014).

External phosphorus loading

Our model showed that externally loaded phosphorus accumulated in the water column of western Lake Erie in both 1997 and 1998, which is consistent with Schwab et al.'s (2009) 3-D hydrodynamics model that simulated the external P distribution over a whole year for 1994. This long retention time may help to explain how phosphorus loaded into Lake Erie in early spring can be a determining factor to predict *Microcystis* blooms later in summer and fall (e.g., Stumpf et al., 2012).

Although our model does not include all tributaries along the lake shore, the major tributaries have been included (Bolsenga and Herdendorf, 1993; Dolan, 1993; Schwab et al., 2009). Furthermore, considering the overwhelming loads from the Maumee River and the Detroit River, our model captures the general character of the external loading to Lake Erie during each summer growing season. Model performance would be improved if P loading data from the Grand River, Ontario, were available (Boegman et al., 2008a, 2008b), as this river is the major source of external nutrient loading to the eastern basin. Due to field data limitations, our simulation periods were from May to September in 1997, and from June to October in 1998, which missed the high P loadings from the Maumee River during January through April (or May in 1998), when a large fraction of the annual loads entered the lake (Fig. 3). The effects of these loads should be captured with our model initial conditions; however, they will not be reduced in the load reduction scenarios.

Internal phosphorus loading

The uncertainty in the relationship between external P loads and *Microcystis* blooms (Obenour et al., 2014) calls for more studies on unknown factors that could play an important role in *Microcystis* dynamics, such as internal P loading (Kane et al., 2014). Our results show that P recycling within the upper water column contributes the major portion to algal demands, with organic matter decay as the primary contributor. Phosphorus pools and pathways in the water column responded faster to the reduction of external P loads than did pathways to the sediment.

Burns and Ross (1972) estimated that the phosphate regeneration rate under oxygenated conditions in the central basin of Lake Erie was 22 μmol P m^{-2} d^{-1} (0.0007 g m^{-2} d^{-1}); while the anoxic regeneration rate was 245 μmol P m^{-2} d^{-1} (0.0076 g m^{-2} d^{-1}). Lam et al. (1983) assumed that the release rate was 0.0044 g m^{-2} d^{-1} under anoxic conditions. We took Lam et al.'s approach and ignored the phosphorus release under oxygenated conditions. Thus, phosphorus release by sediments occurred mainly in the central basin, where seasonal hypoxia occurs. Our estimates should be considered conservative with a relatively low anoxic release rate, in addition to our ignoring the small but significant normoxic release of P in Lake Erie (Matisoff et al., 2016). Sediment release was not available to algae during the stratification period in the central and eastern basins, but will be available after the fall overturn when it may support algal growth. This production will further enhance the net organic matter sedimentation to the bottom, fuel sediment oxygen demand in the central basin in the next year, and delay the reduction of hypoxia in the central basin expected from any external P reduction (IJC, 2014). Our study supports Burns et al.'s (2005) finding that the oxygen depletion rate in the hypolimnion of the central basin was correlated with the previous year's load of total phosphorus. A long-term simulation (e.g., several years) of the ecosystem (including October to May periods) is needed in order to quantitatively estimate this delay in response.

Numerous studies have focused on dreissenid P excretion and its ecological impacts (e.g., Mellina et al., 1995; Arnott and Vanni, 1996; Bierman et al., 2005; Conroy et al., 2005b). Our model showed a zebra mussel population excretion rate lower than Mellina et al.'s (1995) estimates, because the mussel density (220×10^3 ind/m^2) in Mellina et al.'s study was much higher than that in our study (3 to 6×10^3 m^{-2}). Our estimates of mussel P excretion were also at the lower range of Arnott and Vanni's (1996) estimates, but mussel excretion still contributed 19–27% of algal demands in the western basin, with an even higher contribution under lower external loads. Mussel excretion as an internal P source would become more important with increasing mussel populations (Zhang et al., 2011), and a recent survey showed that the dreissenid mussel biomass in western Lake Erie tripled from 1998 to 2011(Karatayev et al., 2014). Mussel excretion is also temperature-dependent (Johengen et al., 2013), while constant excretion rates in our model were measured at the high end of the bottom temperatures. Thus, we may overestimate the mussel phosphorus excretion in this aspect.

Zooplankton excretion is an important phosphorus source in lakes (Hudson et al., 1999; Vanni, 2002; Conroy et al., 2005b). Zooplankton excreta and organic matter release are readily available to algae and dominate the P supply supporting algal production (Carpenter and Kitchell, 1984; Scavia et al., 1988). Our model suggests crustacean excretion provided up to 22% of the algal P demand, which was consistent with Boegman et al.'s (2008b) estimates that zooplankton excretion supported 26% of algal P uptake in 1994. Vanni (2002) estimated zooplankton excretion supports as much as 58% of the primary producer P demand, higher than our estimates.

Phosphorus release from the sediment was less than the P sedimentation losses, which indicates that extra P is accumulated in the lake. However, this study does not simulate sediment resuspension, which may bring a large amount of phosphorus from sediment into the

water column in the western basin (Matisoff and Carson, 2014; T. Johengen, University of Michigan, personal communication). Increases in epilimnion phosphorus in the central basin after fall overturn due to up-mixing of hypolimnion phosphorus and sediment resuspension were well documented for the fall of 1970, and the resultant high concentration lasted for several months (Bunns, 1976; Lam and Jaquet, 1976). Hawley and Eadie (2007) calculated that the top 20–40 mm sediment in the central basin was subject to erosion and deposition on an annual basis. However, large storms (e.g., the November 1940 storm) can resuspend up to 2 m of sediment (Lick et al., 1994). Thus if the settled organic matter is not buried deeply enough on the bottom or there are strong storms, sediment resuspension during storm events can fuel major algal production in the water column. With storms becoming much stronger with climate change, this factor will become more and more important, causing a delay in oligotrophication despite any P loading management plan. However, the phosphorus input from sediment resuspension may be significantly less bioavailable (Matisoff and Carson, 2014) and less influential to algal growth (LimnoTech, 2014; Verhamme et al., 2016b).

Effects of phosphorus reduction on the algal community in the western basin

Our simulation results show a decrease in external P loads is an effective way to control algae, especially the NDIA such as *Microcystis*, and supports the newly announced reduction target in external P load to Lake Erie. Our study shows the dynamics of different algal groups (NDEA, diatoms and NDIA) over the growing seasons and their interactions. In Lake Erie NDIA was dominated by *Microcystis*, so we parameterized the NDIA group as *Microcystis* (Zhang et al., 2008), and we focus on *Microcystis* in this discussion. Diatoms prefer cooler water temperatures and experience higher sinking rates due to their heavy silica frustules, and are often abundant during spring and fall. Thus diatoms do not compete with *Microcystis* severely. However, NDEA have a similar temperature and phosphorus niche to that of *Microcystis*, and showed strong competition interactions with *Microcystis* in our model. *Microcystis* outcompeted NDEA in August and September by decreasing light conditions for NDEA growth. *Microcystis* is less affected by light conditions than its competitors given its capacity of maintaining growth under relative lower light intensity (Reynolds and Walsby, 1975) and by buoyancy regulation (Belov and Giles, 1997). A pulse of nutrient input is often associated with high turbidity (riverine input or sediment resuspension) that can significantly limit NDEA growth. This light condition may be accompanied with the fast growth of *Microcystis* boosted by the P loads when temperature is optimal, as was the case in 1998, when NDEA lost in competition with *Microcystis*. The competition for phosphorus between NDEA and *Microcystis* is not bilaterally equal. *Microcystis* can regulate its buoyancy to locate itself in a water layer with high phosphorus content, and store phosphorus intracellularly for later growth after moving into a water layer with good light conditions (Harke et al., 2016). Once *Microcystis* dominates the community, NDEA loses the competition until temperatures become cool or nutrients are depleted and *Microcystis* declines (Wynne et al., 2010). Another disadvantage to NDEA for this competition is that they are food for zooplankton and mussels, while *Microcystis* is not (Aleya et al., 2006). Although the output of the representative model cell did not show that zooplankton grazing mortality causes significant decreases in NDEA, zooplankton does have a high grazing capacity and causes a late June clear-water phase in many lakes (e.g., Wu and Culver, 1991). Zooplankton grazing may thus contribute to a community shift to *Microcystis* dominance. Dreissenid mussels' selective filtration also promotes *Microcystis* blooms (e.g., Vanderploeg et al., 2001).

The two simulation years in our model had contrasting P loads and *Microcystis* bloom sizes, with high P loads in 1997 but no *Microcystis* bloom and lower P loads in 1998 accompanied by a moderate *Microcystis* bloom, thus the total amount of external P load is not the sole determining factor of *Microcystis* blooms. The timing of external loads can be important, e.g., high loading during July and August of 1998 boosted the growth of *Microcystis*. The output from the representative model cell shows that several consecutive P input pulses occurred immediately before the increase in *Microcystis* biomass, which highlights the importance of timing of nutrient inputs (IJC, 2014). Similarly, Michalak et al. (2013) hypothesized that a strong resuspension event immediately preceding bloom onset was one of the ideal conditions for bloom development. Although they assumed this event will bring more over-wintering *Microcystis* cells from the sediment to the water column, it was also associated with a big P input from the sediment into the water column. Unfortunately, without a clear definition of 'strong,' they rejected this hypothesis later on. Year 1997 could be an outlier in statistical models for prediction of *Microcystis* blooms using external P loads (e.g., Stumpf et al., 2012). However, it does provide us a unique chance to use a different approach to study *Microcystis* blooms and identifies some critical factors that can be incorporated into statistical models and improve their predictions and reduce uncertainty.

Effects of phosphorus reduction on hypoxia in the central basin

Hypoxia has become much stronger (expressed as areal extent and duration) in recent years (Scavia et al., 2014). Our modeling results showed that hypoxia's response to external P loading was similar to that reported by the Annex 4 Resemble Modeling Group (Scavia and DePinto, 2015; Scavia et al., 2016-in this issue). However, the simulated hypoxic area tended to be larger in 1998 under TP load similar to those in their focus year (2008), which is likely a result of differences in meteorology and resulting thermal structure (Rucinski et al., 2014).

Conclusion

We used a 2-D water quality model to study the effects of external and internal P loads on algal dynamics. Our results support the use of a phosphorus reduction program to improve water quality in Lake Erie. Our study indicates that reduction in external phosphorus would result in fast and large decreases in algal biomass and *Microcystis* blooms in the western basin. However, several phosphorus input pulses during physically favorable periods of *Microcystis* net growth can dramatically increase *Microcystis* and consequently decrease the light condition for NDEA and limit NDEA growth, promoting a rapid community shift to *Microcystis* dominance. Central basin hypoxia would likely take a longer time to respond to external phosphorus reduction. Additional factors, such as the spatial distribution of external P loads, the contribution of internal phosphorus loads and sediment resuspension events may delay the occurrence of improved water quality, in part because sediment resuspension and transportation are less responsive to changes in external phosphorus. More studies are needed of long-term cycling of phosphorus in the lake, including the processes in sediment-water interactions.

Acknowledgments

This study was sponsored by grants from the Ohio Lake Erie Office – Lake Erie Protection Fund Project # LEPF 98-17, the Ohio Department of Natural Resources as part of the Federal Aid in Sport Fish Restoration Program (F-69-P, Fish Management in Ohio) administered jointly by the U.S. Fish and Wildlife Service and the Ohio Division of Wildlife, and the US Environmental Protection Agency (GL-97590101). This work was also funded by the US Environmental Protection Agency under contract EP-R5-11-07, Task Order 21, and CILER's Cooperative Agreement, Award Number — NA12OAR4320071. We appreciate the valuable review comments from E.A. Marschall and R.M. Sykes at the Ohio State University, and the three anonymous reviewers on a previous draft of this manuscript. This is NOAA Great Lakes Environmental Research Laboratory contribution 1835.

Appendix A. Supplementary data

Supplementary data to this article can be found online at http://dx.doi.org/10.1016/j.jglr.2016.09.005.

References

Aleya, L., Michard, M., Khattabi, H., Devaux, J., 2006. Coupling of the biochemical composition and calorific content of zooplankters with the *Microcystis aeruginosa* proliferation in a highly eutrophic reservoir. Environ. Technol. 27 (11), 1181–1190.

Andersen, T., Hessen, D.O., 1991. Carbon, nitrogen, and phosphorus content of freshwater zooplankton. Limnol. Oceanogr. 36, 807–814.

Arnott, D.L., Vanni, M.J., 1996. Nitrogen and phosphorus recycling by the zebra mussel (*Dreissena polymorpha*) in the western basin of Lake Erie. Can. J. Fish. Aquat. Sci. 53, 646–659.

Baker, D.B., Confesor, R., Ewing, D.E., Johnson, L.T., Kramer, J.W., Merryfield, B.J., 2014. Phosphorus loading to Lake Erie from the Maumee, Sandusky and Cuyahoga rivers: the importance of bioavailability. J. Great Lakes Res. 40, 502–517.

Beeton, A.M., 2002. Large freshwater lakes: present state, trends, and future. Environ. Conserv. 29, 21–38.

Belov, A.P., Giles, J.D., 1997. Dynamical model of buoyant cyanobacteria. Hydrobiologia 349, 87–97.

Bertram, P.E., 1993. Total phosphorus and dissolved oxygen trends in the central basin of Lake Erie, 1970–1991. J. Great Lakes Res. 19, 224–236.

Bierman, V.J., Kaur, J., DePinto, J.V., Feist, T.J., Dilks, D.W., 2005. Modeling the role of zebra mussels in the proliferation of blue-green algae in Saginaw Bay, Lake Huron. J. Great Lakes Res. 31, 32–55.

Boegman, L., Loewen, M.R., Hamblin, P.F., Culver, D.A., 2001. Application of a two-dimensional hydrodynamic reservoir model to Lake Erie. Can. J. Fish. Aquat. Sci. 58, 858–869.

Boegman, L., Loewen, M.R., Hamblin, P.F., Culver, D.A., 2008a. Vertical mixing and weak stratification over zebra mussel colonies in western Lake Erie. Limnol. Oceanogr. 53, 1093–1110.

Boegman, L., Loewen, M.R., Culver, D.A., Hamblin, P.F., Charlton, M.N., 2008b. Spatial-dynamic modeling of lower trophic levels in Lake Erie: relative impacts of zebra mussels and nutrient loading. J. Environ. Eng. ASCE 134, 456–468.

Bolsenga, S.J., Herdendorf, C.E. (Eds.), 1993. Lake Erie and Lake St. Clair Handbook. Wayne State University Press, Detroit (467 pp.).

Bowie, G.L., Mills, W.B., Porcella, D.B., Campbell, C.L., Pagenkopf, J.R., Rupp, G.L., Johnson, K.M., Chan, P.W.H., Gherini, S.A., 1985. Rates, Constants, and Kinetics Formulations in Surface Water Quality Modeling. U.S. Environmental Protection Agency, Environmental Research Laboratory, Athens, Georgia (EPA/600/3–85/040).

Bridgeman, T.B., Chaffin, J.D., Kane, D.D., Conroy, J.D., Panek, S.E., Armenio, P.M., 2012. From river to lake: phosphorus partitioning and algal community compositional changes in western Lake Erie. J. Great Lakes Res. 38, 90–97.

Burlakova, L.E., Karatayev, A.Y., Pennuto, C., Mayer, C., 2014. Changes in Lake Erie benthos over the last 50 years: historical perspectives, current status, and main drivers. J. Great Lakes Res. 40, 560–573.

Burns, N.M., Ross, C., 1972. Project Hypo—An Introduction. In: Burns, N.M., Ross, C. (Eds.), Project Hypo—An Intensive Study of the Lake Erie Central Basin Hypolimnion and Related Surface Water Phenomena. Canada Centre for Inland Waters, Paper No. 6. United States Environmental Protection Agency, Technical Report, TS-05-71-208-24 (February 1972).

Bunns, N.M., 1976. Temperature, oxygen, and nutrient distribution patterns in Lake Erie, 1970. J. Fish. Res. Board Can. 33, 485–511.

Burns, N.M., Rockwell, D.C., Bertram, P.E., Dolan, D.M., Ciborowski, J.J.H., 2005. Trends in temperature, Secchi depth, and dissolved oxygen depletion rates in the central basin of Lake Erie, 1983–2002. J. Great Lakes Res. 31, 35–49.

Carpenter, S.R., Kitchell, J.F., 1984. Plankton community structure and limnetic primary production. Am. Nat. 124, 159–172.

Chapra, S.C., Canale, R.P., 1991. Long-term phenomenological model of phosphorus and oxygen for stratified lakes. Water Res. 25, 707–715.

Chapra, S.C., Robertson, A., 1977. Great Lakes eutrophication: the effect of point source control of total phosphorus. Science 196, 1448–1450.

Cole, T.M., Buchak, E.M., 1995. CE-QUAL-W2: A Two-dimensional, Laterally Averaged, Hydrodynamic and Water Quality Model, Version 2.0: User Manual. Instruction Report EL-95-1. US Army Corps of Engineers, Washington, DC (20314–1000).

Conroy, J.D., Kane, D.D., Dolan, D.M., Edwards, W.J., Charlton, M.N., Culver, D.A., 2005a. Temporal Trends in Lake Erie Plankton Biomass: Roles of External Phosphorus Loading and Dreissenid Mussels. In: Matisoff, G., Ciborowski, J.J.H. (Eds.), Lake Erie Trophic Status Collaborative Study. J. Great Lakes Res. 31(Supplement 2), pp. 89–110.

Conroy, J.D., Edwards, W.J., Pontius, R.A., Kane, D.D., Zhang, H., Shea, J.F., Richey, J.N., Culver, D.A., 2005b. Soluble nitrogen and phosphorus excretion of exotic freshwater mussels (*Dreissena* spp.): potential impacts for nutrient remineralization in western Lake Erie. Freshw. Biol. 50, 1146–1162.

Conroy, J.D., Boegman, L., Zhang, H.Y., Edwards, W.J., Culver, D.A., 2011. "Dead Zone" dynamics in Lake Erie: the importance of weather and sampling intensity for calculated hypolimnetic oxygen depletion rates. Aquat. Sci. 73, 289–304.

DeBruyn, J.M., Leigh-Bell, J.A., McKay, R.M.L., Bourbonniere, R.A., Wilhelm, S.W., 2004. Microbial distributions and the impact of phosphorus on bacterial activity in Lake Erie. J. Great Lakes Res. 30, 166–183.

Di Toro, D.M., Connolly, J.P., 1980. Mathematical Models of Water Quality in Large Lakes. Part 2: Lake Erie. USEPA, Office of Research and Development, ERL-Duluth, LLRS, Grosse Ile, MI. EPA Ecological Research Series EPA-600/3–80-065.

Dolan, D.M., 1993. Point source loadings of phosphorus to Lake Erie: 1986–1990. J. Great Lakes Res. 19, 212–223.

Fennel, W., Neumann, T., 2003. Variability of copepods as seen in a coupled physical–biological model of the Baltic Sea. ICES Mar. Sci. Symp. 219, 208–219.

Gopalan, G., Culver, D.A., Wu, L., Trauben, B.K., 1998. Effects of recent ecosystem changes on the recruitment of young-of-the-year fish in western Lake Erie. Can. J. Fish. Aquat. Sci. 55, 2572–2579.

Harke, M.J., Davis, T.W., Watson, S.B., Gobler, C.J., 2016. Nutrient-controlled niche differentiation of western Lake Erie cyanobacterial populations revealed via metatranscriptomic surveys. Environ. Sci. Technol. 50, 604–615.

Hawley, N., Eadie, B.J.l., 2007. Observations of sediment transport in Lake Erie during the winter of 2004–2005. J. Great Lakes Res. 33, 816–827.

Hecky, R.E., Smith, R.E.H., Barton, D.R., Guildford, S.J., Taylor, W.D., Charlton, M.N., Howell, T., 2004. The nearshore phosphorus shunt: a consequence of ecosystem engineering by dreissenids in the Laurentian Great Lakes. Can. J. Fish. Aquat. Sci. 61, 1285–1293.

Hudson, J.J., Taylor, W.D., Schindler, D.W., 1999. Planktonic nutrient regeneration and cycling efficiency in temperate lakes. Nature 400, 659–661.

IJC (International Joint Commission), 2014. A Balanced Diet for Lake Erie: Reducing Phosphorus Loadings and Harmful Algal Blooms. Report of the Lake Erie Ecosystem Priority (http://www.ijc.org/en_/leep/report).

James, W.F., Barko, J.W., Eakin, H.L., 1997. Nutrient regeneration by the zebra mussel (*Dreissena polymorpha*). J. Freshw. Ecol. 12, 209–216.

Jarvis, P., Dow, J., Dermott, R., Bonnell, R., 2000. Zebra (*Dreissena polymorpha*) and quagga mussel (*Dreissena bugensis*) distribution and density in Lake Erie, 1992–1998. Can. Tech. Rep. Fish. Aquat. Sci. 2304 (46 pp.).

Jin, X., 2003. Analysis of eutrophication state and trend for lakes in China. J. Limnol. 62, 60–66.

Johengen, T.H., Vanderploeg, H.A., Liebig, J.R., 2013. Effects of Algal Composition, Seston Stoichiometry, and Feeding Rate on Zebra Mussel (*Dreissena polymorpha*) Nutrient Excretion in Two Laurentian Great Lakes. In: Nalepa, T.F., Schlosser, D.W. (Eds.), Quagga and Zebra Mussels: Biology, Impacts, and Control, second ed. CRC Press, Boca Raton, FL, pp. 445–459.

Kane, D.D., Conroy, J.D., Peter Richards, R., Baker, D.B., Culver, D.A., 2014. Re-eutrophication of Lake Erie: correlations between tributary nutrient loads and phytoplankton biomass. J. Great Lakes Res. 40, 496–501.

Karatayev, A.Y., Burlakova, L.E., Pennuto, C., Ciborowski, J., Karatayev, V.A., Juette, P., Clapsadl, M., 2014. Twenty five years of changes in *Dreissena* spp. populations in Lake Erie. J. Great Lakes Res. 40, 550–559.

Knoll, L.B., Vanni, M.J., Renwick, W.H., 2003. Phytoplankton primary production and photosynthetic parameters in reservoirs along a gradient of watershed land use. Limnol. Oceanogr. 48, 608–617.

Krieger, K.A., Schloesser, D.W., Manny, B.A., Trisler, C.E., Heady, S.E., Ciborowski, J.J.H., Muth, K.M., 1996. Recovery of burrowing mayflies (Ephemeroptera: Ephemeridae: *Hexagenia*) in western Lake Erie. J. Great Lakes Res. 22, 254–263.

Lam, D.C.L., Jaquet, J.M., 1976. Computations of physical transport and regeneration of phosphorus in Lake Erie, fall 1970. J. Fish. Res. Board Can. 33, 550–563.

Lam, D.C.L., Schertzer, W.M., Fraser, A.S., 1983. Simulation of Lake Erie Water Quality Responses to Loading and Weather Variations. Scientific Series No. 134. National Water Research Institute, Inland Waters Directorate, Canada Center for Inland Waters, Burlington, Ontario.

Lam, D.C., Schertzer, W.M., Fraser, A.S., 1987. Oxygen depletion in Lake Erie: modeling the physical, chemical, and biological interactions, 1972 and 1979. J. Great Lakes Res. 13, 770–781.

Lean, D.R., 1973. Phosphorus dynamics in lake water. Science 179, 678–680.

Lick, W., Lick, J., Ziegler, C.K.l., 1994. The resuspension and transport of fine-grained sediments in Lake Erie. J. Great Lakes Res. 20, 599–612.

LimnoTech, 2014. Influence of Open-lake Placement of Dredged Material on Western Lake Erie Basin Harmful Algal Blooms. UCACE Project W912P4-10-D-0002, Final Study Report, Ann Arbor, MI.

Loewen, M.R., Ackerman, J.D., Hamblin, P.F.l., 2007. Environmental implications of stratification and turbulent mixing in a shallow lake basin. Can. J. Fish. Aquat. Sci. 64, 43–57.

Lucas, A.M., Thomas, N.A., 1972. Sediment Oxygen Demand in Lake Erie's Central basin, 1970. In: Burns, N.M., Ross, C. (Eds.), Project Hypo—An Intensive Study of the Lake Erie Central Basin Hypolimnion and Related Surface Water Phenomena. Canada Centre for Inland Waters, Paper No. 6. United States Environmental Protection Agency, Technical Report, TS-05-71-208-24 (February, 1972).

Ludsin, S.A., Kershner, M.W., Blocksom, K.A., Knight, R.L., Stein, R.A., 2001. Life after death in Lake Erie: nutrient controls drive fish species richness, rehabilitation. Ecol. Appl. 11, 731–746.

Makarewicz, J.C., Bertram, P., 1991. Evidence for the restoration of the Lake Erie North America ecosystem: water quality oxygen levels and pelagic function appear to be improving. Bioscience 41, 216–223.

Matisoff, G., Carson, M.L., 2014. Sediment resuspension in the Lake Erie nearshore. J. Great Lakes Res. 40, 532–540.

Matisoff, G., Kaltenberg, E.M., Steely, R.L., Hummel, S.K., Seo, J., Gibbons, K.J., Bridgeman, T.B., Seo, Y., Behbahani, M., James, W.F., Johnson, L.T., Doan, P., Dittrich, M., Evans, M.A., Chaffin, J.D., 2016. Internal loading of phosphorus in western Lake Erie. J. Great Lakes Res. 42, 775–788.

Mellina, E., Rasmussen, J.B., Mills, E.L., 1995. Impact of zebra mussel (*Dreissena polymorpha*) on phosphorus cycling and chlorophyll in lakes. Can. J. Fish. Aquat. Sci. 52, 2553–2573.

Michalak, A.M., Anderson, E.J., Beletsky, D., Boland, S., Bosch, N.S., Bridgeman, T.B., Chaffin, J.D., Cho, K., Confesor, R., Daloglu, I., DePinto, J.V., Evans, M.A., Fahnenstiel, G.L., He,

L.L., Ho, J.C., Jenkins, L., Johengen, T.H., Kuo, K.C., LaPorte, E., Liu, X.J., McWilliams, M.R., Moore, M.R., Posselt, D.J., Richards, R.P., Scavia, D., Steiner, A.L., Verhamme, E., Wright, D.M., Zagorski, M.A., 2013. Record-setting algal bloom in Lake Erie caused by agricultural and meteorological trends consistent with expected future conditions. Proc. Natl. Acad. Sci. U. S. A. 110, 6448–6452.

Mortimer, C.H., 1941. The exchange of dissolved substances between mud and water in lakes (parts I and II). J. Ecol. 29, 280–329.

Mortimer, C.H., 1971. Chemical exchanges between sediments and water in the Great Lakes — speculations on probable regulatory mechanisms. Limnol. Oceanogr. 16, 387–404.

Obenour, D.R., Gronewold, A.D., Stow, C.A., Scavia, D., 2014. Using a Bayesian hierarchical model to improve Lake Erie cyanobacteria bloom forecasts. Water Resour. Res. 50, 7847–7860.

Patterson, M.W.R., Ciborowski, J.J.H., Barton, D.R., 2005. The distribution and abundance of *Dreissena* species (Dreissenidae) in Lake Erie, 2002. J. Great Lakes Res. 31 (Suppl. 2), 223–237.

Phillips, G., Kelly, A., Pitt, J., Sanderson, R., Taylor, E., 2005. The recovery of a very shallow eutrophic lake, 20 years after the control of effluent derived phosphorus. Freshw. Biol. 50, 1628–1638.

Reynolds, C.S., Walsby, A.E., 1975. Water-blooms. Biol. Rev. 50, 437–481.

Rockwell, D.C., Salisbury, D.K., Lesht, B.M., 1989. Water Quality in the Middle Great Lakes: Results of the 1985 USEPA Survey of Lakes Erie, Huron and Michigan. Rep. No. EPA 605/6-89-001. U.S. Environmental Protection Agency, Great Lakes National Program Office, 230 South Dearborn, Chicago, IL 60604.

Rucinski, D.K., DePinto, J.V., Scavia, D., Beletsky, D., 2014. Modeling Lake Erie's hypoxia response to nutrient loads and physical variability. J. Great Lakes Res. 40, 151–161.

Scavia, D., Chapra, S.C., 1977. Comparison of an ecological model of Lake Ontario and phosphorus loading models. J. Fish. Res. Board Can. 34, 286–290.

Scavia, D., DePinto, J.V., 2015. Great Lakes water quality agreement nutrient annex objectives and targets task team ensemble modeling report. http://tinyurl.com/ng6d3tn (Viewed 12 April 2016).

Scavia, D., Lang, G.A., Kitchell, J.F., 1988. Dynamics of Lake Michigan plankton: a model evaluation of nutrient loading, competition, and predation. Can. J. Fish. Aquat. Sci. 45, 165–177.

Scavia, D., David, A.J., Arend, K.K., Bartell, S., Beletsky, D., Bosch, N.S., Brandt, S.B., Briland, R.D., Daloğlu, I., DePinto, J.V., Dolan, D.M., Evans, M., Farmer, T.M., Goto, D., Han, H., Höök, T.O., Knight, R., Ludsin, S.A., Mason, D., Michalak, A.M., Richards, P.R., Roberts, J.J., Rucinski, D.K., Rutherford, E., Schwab, D.J., Sesterhenn, T.M., Zhang, H., Zhou, Y., 2014. Assessing and addressing the re-eutrophication of Lake Erie: central basin hypoxia. J. Great Lakes Res. 40, 226–246.

Scavia, D., DePinto, J.V., Bertani, I., 2016. A multi-model approach to evaluating target phosphorus loads for Lake Erie. J. Great Lakes Res. 42, 1139–1150 (in this issue).

Schindler, D.W., 1977. Evolution of phosphorus limitation in lakes. Science 195, 260–262.

Schindler, D.W., 2012. The dilemma of controlling cultural eutrophication of lakes. Proc. R. Soc. B Biol. Sci. http://dx.doi.org/10.1098/rspb.2012.1032.

Schwab, D.J., Beletsky, D., DePinto, J., Dolan, D.M., 2009. A hydrodynamic approach to modeling phosphorus distribution in Lake Erie. J. Great Lakes Res. 35, 50–60.

Smith, V.H., 1982. The nitrogen and phosphorus dependence of algal biomass in lakes: an empirical and theoretical analysis. Limnol. Oceanogr. 27, 1101–1112.

Stoeckmann, A., 2003. Physiological energetics of Lake Erie dreissenid mussels: a basis for the displacement of *Dreissena polymorpha* by *Dreissena bugensis*. Can. J. Fish. Aquat. Sci. 60, 126–134.

Stumpf, R.P., Wynne, T.T., Baker, D.B., Fahnenstiel, G.L., 2012. Interannual variability of cyanobacterial blooms in Lake Erie. PLoS One 7 (8), e42444.

Turner, R.E., Rabalais, N.N., Justic, D.I., 2008. Gulf of Mexico hypoxia: alternate state and a legacy. Environ. Sci. Technol. 42, 2323–2327.

US EPA, 2016. News release: governments of Canada and the United States announce phosphorus reduction targets of 40 percent to improve Lake Erie water quality and reduce public health risk. Downloaded 8 May from [2016yosemite epa.gov/opa/admpress.nsf/d0cf6618525a9efb85257359003fb69d/d6fb4cb50080797585257f610067d8bd!OpenDocument.

Vanderploeg, H.A., Liebig, J.R., Carmichael, W.W., Age, M.A., Johengen, T.H., Fahnenstiel, G.L., Nalepa, T.F., 2001. Zebra mussel (*Dreissena polymorpha*) selective filtration promoted toxic *Microcystis* blooms in Saginaw Bay (Lake Huron) and Lake Erie. Can. J. Fish. Aquat. Sci. 58, 1208–1221.

Vanderploeg, H., Sarnelle, O., Liebig, J.R., Morehead, N.R., Robinson, S.D., Johengen, T., Horst, G.P., 2016. Seston nutrient stoichiometry drives feeding, tissue nutrient stoichiometry, and excretion in zebra mussels. Freshw. Biol. (in review).

Vanni, M.J., 2002. Nutrient cycling by animals in freshwater ecosystems. Ann. Rev. Ecol. Syst. 33, 341–370.

Verhamme, E.M., Redder, T., Schlea, D., Grush, J., Bratton, J.F., DePinto, J.V., 2016a. Development of the western Lake Erie Ecosystem Model (WLEEM): application to connect phosphorus loads to cyanobacteria biomass. J. Great Lakes Res. 42, 1193–1205 (in this issue).

Verhamme, E., Bratton, J., DePinto, J., Redder, T., Schlea, D., 2016b. Western Lake Erie Ecosystem Model (WLEEM) Phosphorus Mass Balance and Sediment Flux. Report. LimnoTech, Inc., Ann Arbor, MI.

Wetzel, R.G. (Ed.), 2001. Limnology, 3rd edition Academic Press, San Diego, CA (1006 pp.).

Wilhelm, S.W., DeBruyn, J.M., Gillor, O., Twiss, M.R., Livingston, K., Bourbonniere, R.A., Pickell, L.D., Trick, C.G., Dean, A.L., McKay, R.M.L., 2003. Effect of phosphorus amendments on present day plankton communities in pelagic Lake Erie. Aquat. Microb. Ecol. 32 (3), 275–285.

Wu, L., Culver, D.A., 1991. Zooplankton grazing and phytoplankton abundance — an assessment before and after invasion of *Dreissena polymorpha*. J. Great Lakes Res. 17, 425–436.

Wynne, T.T., Stumpf, R.P., Tomlinson, M.C., Dyble, J., 2010. Characterizing a cyanobacterial bloom in western Lake Erie using satellite imagery and meteorological data. Limnol. Oceanogr. 55, 2025–2036.

Young, T.C., DePinto, J.V., Flint, S.E., Switzenbaum, M.S., Edzwald, J.K., 1982. Algal availability of phosphorus in municipal wastewater. J. Water Pollution Control Fed. 54, 1505–1516.

Zhang, H., Culver, D.A., Boegman, L., 2008. A two-dimensional ecological model of Lake Erie: application to estimate dreissenid impacts on large lake plankton populations. Ecol. Model. 214, 219–241.

Zhang, H.Y., Culver, D.A., Boegman, L., 2011. Dreissenids in Lake Erie: an algal filter or a fertilizer? Aquat. Invasions 6, 175–194.

Zhou, Y., Obenour, D.R., Scavia, D., Johengen, T.H., Michalak, A.M., 2013. Spatial and temporal trends in Lake Erie hypoxia, 1987–2007. Environ. Sci. Technol. 47, 899–905. http://dx.doi.org/10.1021/es303401b.